

NASA/CR-2011-217161



Edgewise Compression Testing of STIPS-0 (Structurally Integrated Thermal Protection System)

Amy R. Brewer
Analytical Services and Materials, Inc., Hampton, Virginia

July 2011

NASA STI Program . . . in Profile

Since its founding, NASA has been dedicated to the advancement of aeronautics and space science. The NASA scientific and technical information (STI) program plays a key part in helping NASA maintain this important role.

The NASA STI program operates under the auspices of the Agency Chief Information Officer. It collects, organizes, provides for archiving, and disseminates NASA's STI. The NASA STI program provides access to the NASA Aeronautics and Space Database and its public interface, the NASA Technical Report Server, thus providing one of the largest collections of aeronautical and space science STI in the world. Results are published in both non-NASA channels and by NASA in the NASA STI Report Series, which includes the following report types:

- **TECHNICAL PUBLICATION.** Reports of completed research or a major significant phase of research that present the results of NASA programs and include extensive data or theoretical analysis. Includes compilations of significant scientific and technical data and information deemed to be of continuing reference value. NASA counterpart of peer-reviewed formal professional papers, but having less stringent limitations on manuscript length and extent of graphic presentations.
- **TECHNICAL MEMORANDUM.** Scientific and technical findings that are preliminary or of specialized interest, e.g., quick release reports, working papers, and bibliographies that contain minimal annotation. Does not contain extensive analysis.
- **CONTRACTOR REPORT.** Scientific and technical findings by NASA-sponsored contractors and grantees.

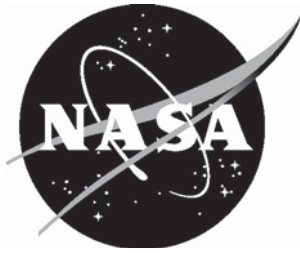
- **CONFERENCE PUBLICATION.** Collected papers from scientific and technical conferences, symposia, seminars, or other meetings sponsored or co-sponsored by NASA.
- **SPECIAL PUBLICATION.** Scientific, technical, or historical information from NASA programs, projects, and missions, often concerned with subjects having substantial public interest.
- **TECHNICAL TRANSLATION.** English-language translations of foreign scientific and technical material pertinent to NASA's mission.

Specialized services also include creating custom thesauri, building customized databases, and organizing and publishing research results.

For more information about the NASA STI program, see the following:

- Access the NASA STI program home page at <http://www.sti.nasa.gov>
- E-mail your question via the Internet to help@sti.nasa.gov
- Fax your question to the NASA STI Help Desk at 443-757-5803
- Phone the NASA STI Help Desk at 443-757-5802
- Write to:
NASA STI Help Desk
NASA Center for AeroSpace Information
7115 Standard Drive
Hanover, MD 21076-1320

NASA/CR-2011-217161



Edgewise Compression Testing of STIPS-0 (Structurally Integrated Thermal Protection System)

Amy R. Brewer
Analytical Services and Materials, Inc., Hampton, Virginia

National Aeronautics and
Space Administration

Langley Research Center
Hampton, Virginia 23681-2199

Prepared for Langley Research Center
under Contract NNL09AM18T

July 2011

The use of trademarks or names of manufacturers in this report is for accurate reporting and does not constitute an official endorsement, either expressed or implied, of such products or manufacturers by the National Aeronautics and Space Administration.

Available from:

NASA Center for Aerospace Information
7115 Standard Drive
Hanover, MD 21076-1320
443-757-5802

TABLE OF CONTENTS

TABLE OF CONTENTS	I
LIST OF TABLES	II
LIST OF FIGURES	II
ACKNOWLEDGEMENTS.....	III
NOMENCLATURE.....	IV
ABSTRACT.....	1
1. INTRODUCTION.....	1
2. SITPS-0 TEST ARTICLE	2
3. EDGEWISE COMPRESSION TEST SETUP.....	4
3.1. SPECIMEN POTTING	4
3.2. SPECIMEN INSTRUMENTATION.....	5
3.2.1. DCDTs (<i>Out-of-Plane Displacements</i>).....	6
3.2.2. Strain Gages (<i>In-Plane Strain and Poisson's Ratio</i>)	7
3.2.3. Photogrammetry (<i>In-Plane Strain, Out-of-Plane Displacements</i>)	8
3.2.4. Acoustic Emission Sensors (<i>Damage Indicator</i>).....	9
3.3. TEST STAND	10
3.4. TEST SEQUENCE.....	11
4. TEST RESULTS.....	12
4.1. COMPRESSIVE ELASTIC MODULUS	12
4.2. PROPORTIONAL LIMIT	13
4.3. POISSON'S RATIO	14
4.4. BENDING / OUT-OF-PLANE DISPLACEMENTS	15
4.4.1. DCDTs.....	15
4.4.2. Photogrammetry.....	18
4.4.3. Acoustic Emission	19
4.5. IN-PLANE STRAINS	20
4.5.1. Longitudinal Strain Gages	20
4.5.2. Photogrammetry.....	22
4.6. POST-TEST NON-DESTRUCTIVE EVALUATION	22
4.6.1. Thermography Image of Delamination.....	22
4.6.2. Computed Tomography (CT)	23
5. CONCLUSIONS	25
REFERENCES.....	26
APPENDIX A: IML OUT-OF-PLANE DISPLACEMENTS (PHOTOGRAMMETRY)	27
APPENDIX B: POST-TEST CT IMAGES.....	31
B.1 VOIDS AT OVERWRAP INTERSECTIONS	32
B.2 THROUGH PANEL THICKNESS - CT IMAGES OF SITPS-0	33
B.3 THROUGH PANEL DEPTH - CT IMAGES OF SITPS-0.....	40

LIST OF TABLES

TABLE 1. EDGEWISE COMPRESSION LOADING SEQUENCE	11
TABLE 2. COMPRESSIVE ELASTIC MODULUS	13
TABLE 3. POISSON'S RATIO	15

LIST OF FIGURES

FIGURE 1. SITPS TEST ARTICLE	2
FIGURE 2. AETB ORIENTATION OF SITPS-0 AETB BARS	3
FIGURE 3. SURFACE ANOMALIES FROM APPLIED INSTRUMENTATION FOR THERMAL TESTING.....	4
FIGURE 4. REQUESTED POTTING GEOMETRY (DIMENSION IN INCHES)	5
FIGURE 5. INSTRUMENTED SITPS-0 TEST ARTICLE IN TEST LOAD FRAME	6
FIGURE 6. INSTRUMENTATION LAYOUT.....	6
FIGURE 7. DCDT LAYOUT FOR BENDING AND OUT-OF-PLANE DISPLACEMENTS.....	7
FIGURE 8. STRAIN GAGE LOCATIONS FOR IN-PLANE STRAINS	8
FIGURE 9. PHOTOGRAMMETRY SYSTEM SETUP.....	9
FIGURE 10. ACOUSTIC EMISSION SENSOR LOCATION	10
FIGURE 11. SOUTHWARK EMERY 120-KIP TEST STAND	11
FIGURE 12. SITPS-0 STRESS-STRAIN CURVES (PSI)	13
FIGURE 13. SITPS-0 PROPORTIONAL LIMIT (OFFSET = -5.0 $\mu\epsilon$)	14
FIGURE 14. ROSETTE STRAIN GAGE RESPONSE USED TO CALCULATE POISSON'S RATIO FOR EACH FACESHEET .	15
FIGURE 15. DCDT OUT-OF-PLANE DISPLACEMENT SIGN CONVENTION.....	16
FIGURE 16. OUT-OF-PLANE DISPLACEMENT (DCDT) - 10K LOADING SEQUENCE	16
FIGURE 17. OUT-OF-PLANE DISPLACEMENT (DCDT) - 20K LOADING SEQUENCE	17
FIGURE 18. OUT-OF-PLANE DISPLACEMENTS (DCDT) – 37K LOADING SEQUENCE	17
FIGURE 19. OVERVIEW OF OUT-OF-PLANE DISPLACEMENTS @ 37K LBS.....	18
FIGURE 20. OUT-OF-PLANE DISPLACEMENTS AT P = 37K LBS (PHOTOGRAMMETRY SYSTEM)	19
FIGURE 21. ACOUSTIC EMISSION - FIRST ARRIVAL OCCURRENCES	20
FIGURE 22. IN-PLANE STRAINS (STRAIN GAGE DATA)	21
FIGURE 23. IN-PLANE STRAINS AT P = 37K LBS (PHOTOGRAMMETRY SYSTEM)	22
FIGURE 24. THERMOGRAPHY IMAGE OF IML SHOWING DELAMINATION.....	23
FIGURE 25. POST-TEST CT IMAGES	24
FIGURE A-1: PHOTOGRAMMETRY IMAGE (FRAME) WITH RESPECT TO STRESS-STRAIN CURVE	27
FIGURE A-2. PHOTOGRAMMETRY IMAGES	28
FIGURE B-1. VIEWING ORIENTATION FOR CT IMAGES	31
FIGURE B-2. VOIDS AT AETB OVERWRAP INTERSECTIONS	32
FIGURE B-3. THROUGH PANEL THICKNESS - CT IMAGES OF SITPS-0	33
FIGURE B-4. THROUGH PANEL DEPTH - CT IMAGES OF SITPS-0.....	40

Hi-Nicalon™ is a trademark of COI Ceramic, Incorporated, 7812 West 4100 South, Magna, Utah 84044.

ACKNOWLEDGEMENTS

The author would like to thank the following groups for their contributions to the SITPS Program.

- The Hypersonics Program of Fundamental Aeronautics for their contribution to the SITPS program,
- The SITPS Team at NASA for oversight and participation in the development of the SITPS Concept and
- The Structural Mechanics and Concepts Branch test facility at Langley Research Center for test resources and oversight.

In particular, the author would like to thank the following persons for their contributions to the testing and evaluation of the SITPS-0 panel.

- Jeff Gragg of NASA Langley Research Center (LaRC-D326) for his participation in the testing of the SITPS test article,
- Matt Moholt of NASA Dryden Flight Research Center (DFRC-RS) for his participation in testing of the SITPS-0 test article,
- Patrick McNeil of Analytical Sciences & Material, Inc. at NASA Langley Research Center (LaRC-D312) for the Photogrammetry work, and
- The NDE Group at NASA Langley Research Center (LaRC-D313): Patty Howell for Thermography, Eric Burke for Computed Tomography, Eric Madaras and Michael Horne for Acoustic Emission,
- Kim Bey and Sandra Walker of NASA Langley Research Center (LaRC-D312) for their participation in editions of this document.

NOMENCLATURE

8HS	eight Harness Satin weave
A.....	cross-sectional area (in ²)
AETB.....	Alumina Enhanced Thermal Barrier
CT	Computed Tomography
DCDT	Direct Current Displacement Transducer
E.....	elastic modulus (psi)
IML	Inner Mold Line (M55J/954-3 Cyanate Ester)
OML	Outer Mold Line (S200Hm)
P.....	compressive load (lb)
PIP	Polymer Impregnation and Pyrolysis
S200Hm	modified S200H facesheet
SG.....	Strain gage
SITPS.....	Structurally Integrated Thermal Protection System
ϵ	engineering strain (in/in)
ϵ_L	longitudinal strain (in/in)
ϵ_T	transverse strain (in/in)
ϵ_{prop}	engineering strain (in/in) at proportional limit
σ	engineering stress (psi)
σ_{prop}	engineering stress (psi) at proportional limit
ν	Poisson's ratio

ABSTRACT

The Structurally Integrated Thermal Protection System (SITPS) task was initiated by the NASA Hypersonics Project under the Fundamental Aeronautics Program to develop a structural load-carrying thermal protection system for use in aerospace applications. The initial NASA concept for SITPS consists of high-temperature composite facesheets (outer and inner mold lines) with a light-weight insulated structural core.⁽¹⁾

An edgewise compression test was performed on the SITPS-0 test article at room temperature using conventional instrumentation and methods in order to obtain panel-level mechanical properties and behavior of the panel.

Three compression loadings (10, 20 and 37 kips) were applied to the SITPS-0 panel. The panel behavior was monitored in-situ using standard techniques and non-destructive evaluation (NDE) methods such as photogrammetry and acoustic emission. The elastic modulus of the SITPS-0 panel was determined to be 1.146×10^6 psi with a proportional limit at 1039 psi. Barrel-shaped bending of the panel and partial delamination of the IML occurred under the final loading. The delamination was verified post-testing using thermography. The panel was also imaged with Computed Tomography (CT) post-testing.

1. INTRODUCTION

The Structurally Integrated Thermal Protection System (SITPS) task was initiated by the NASA Hypersonics Project under the Fundamental Aeronautics Program to develop a structural load-carrying thermal protection system for use in aerospace applications. The initial NASA concept for SITPS consists of high-temperature composite facesheets (outer and inner mold lines) with a light-weight insulated structural core.⁽¹⁾

The Structurally Integrated Thermal Protection System (SITPS) concept provides an integrated structural component designed to carry both aerodynamic and thermal loads. The inner and outer walls carry the aerodynamic loading. The outer wall operates at high temperatures typical of hypersonic re-entry. The thermally-insulative inner core will provide thermal protection through the thickness of the system which maintains the inner surface at below acceptable maximum temperatures.

An edgewise compression test was performed on the SITPS-0 test article at room temperature using conventional instrumentation and methods in order to obtain panel-level mechanical properties and behavior of the panel. Of particular interest were the basic mechanical properties of the test article including the elastic modulus, proportional limit and Poisson's Ratio.

2. SITPS-0 TEST ARTICLE

The as-fabricated test article, SITPS-0 panel, is shown Figure 1. The SITPS-0 panel measured approximately 11.5" x 11.5" x 2.25" thick and the recorded area weight is 5.8 lbs/ft².

The SITPS-0 core consists of two orthogonal layers of eleven 1-inch x1-inch AETB-16 (alumina enhanced thermal barrier) bars. The AETB-16 bars were individually spiral wrapped with Hi-NicalonTM/SiNC (Hi-Nic, 2D 8HS weave composite, 30°, 1-ply, 0.0125-inch). The AETB and Hi-NicalonTM/SiNC fabrication protocol are not available at this time (proprietary).

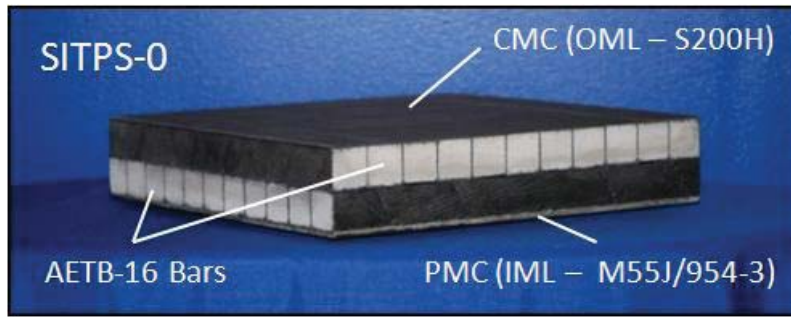
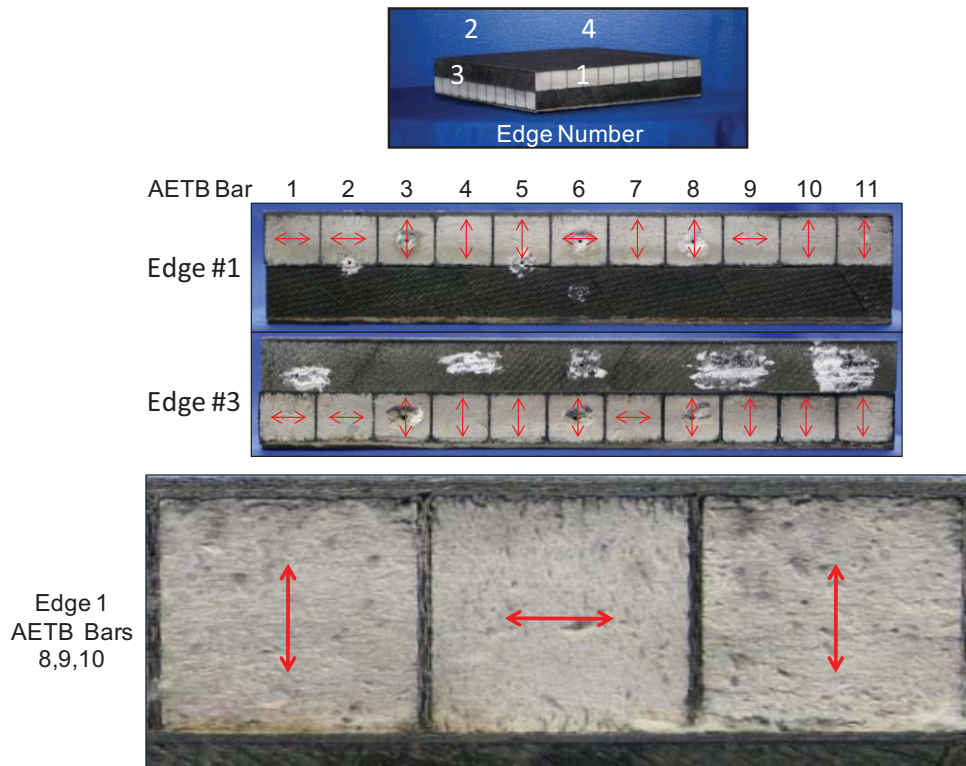


Figure 1. SITPS Test Article

The outer mold line (OML) is S200Hm SiC/SiC 2D 8HS ceramic matrix composite ([0]₆, 0.075"). The layers of fabric forming the OML were green and were adhered to the AETB bar core prior to densification; therefore, densification of the OML occurred from the free face side only. The Polymer Impregnation and Pyrolysis (PIP) methodology was used for densification of the OML and AETB-16 bar assembly (9-cycles) with painting of the exposed surfaces between PIP cycles.

The inner mold line (IML) is a M55J/954-3 Cyanate Ester tape (8-ply, [0/45/-45/90], 0.096-inch). The IML was fabricated and cured by COI Ceramics, Inc. The cured IML was bonded to the SITPS-0 panel with FM-300 adhesive after completion of the densification process of the OML and AETB bar assembly.

The orientation of each AETB bar in the SITPS-0 panel is shown in Figure 2. The thermal and mechanical properties of AETB are different in the through-thickness and in-plane directions, therefore orientation is important. The exposed edges of each AETB bar (Edges #1 through #4) were visually inspected for the AETB orientation, the through-thickness direction is orthogonal to the fiber direction. Edges #1 and #3 are shown and the arrows indicate the AETB through-thickness direction. The bottom figure shows AETB bar 8, 9 and 10 of Edge #1.



**Figure 2. AETB Orientation of SITPS-0 AETB Bars
(Magnification of Edge #1 - AETB bars 8, 9, and 10)
(Preferred orientation is \updownarrow through thickness)**

Prior to mechanical testing, the SITPS-0 test article was subjected to thermal testing.⁽²⁾ The thermal testing required that several thermocouples be inserted into the AETB-16 material which resulted in gouges in the AETB-16 shown in Figures 2 and 3 (Figure 3 designated by \circ). The white residue on the overwraps and the OML in Figures 2 and 3 is residue from glue that held the thermocouple wires in place.

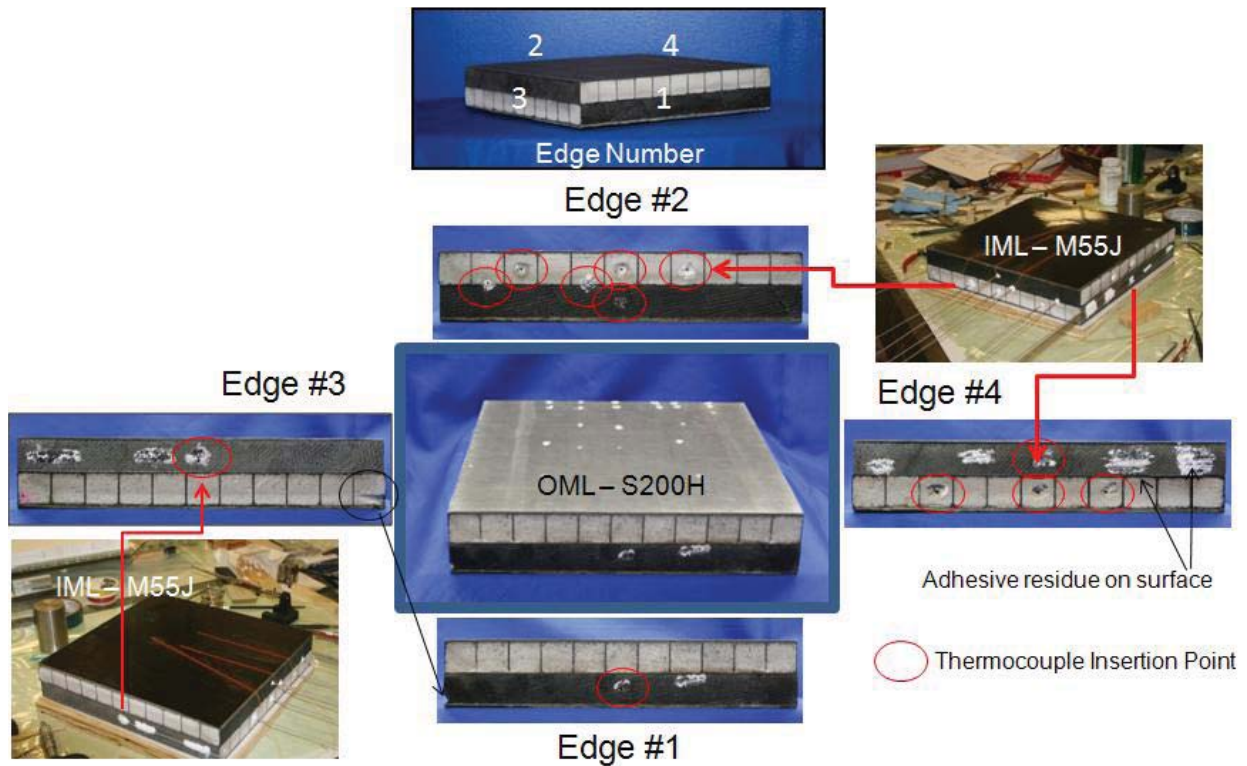


Figure 3. Surface Anomalies from Applied Instrumentation for Thermal Testing

3. EDGEWISE COMPRESSION TEST SETUP

3.1. Specimen Potting

The panel ends were potted using a 1-inch form and Unisorb V100 potting material. The specimen and forms were positioned such that the potting enclosed the ends of specimen and the potting material was to extend outside the 1-inch form. After potting, the top and bottom surfaces of the potting medium were machined or ground such that the potted surfaces were flat and parallel to within ± 0.001 -in. of each other, and potting surfaces were perpendicular to the specimen. The requested potting layout is shown in the Figure 4.

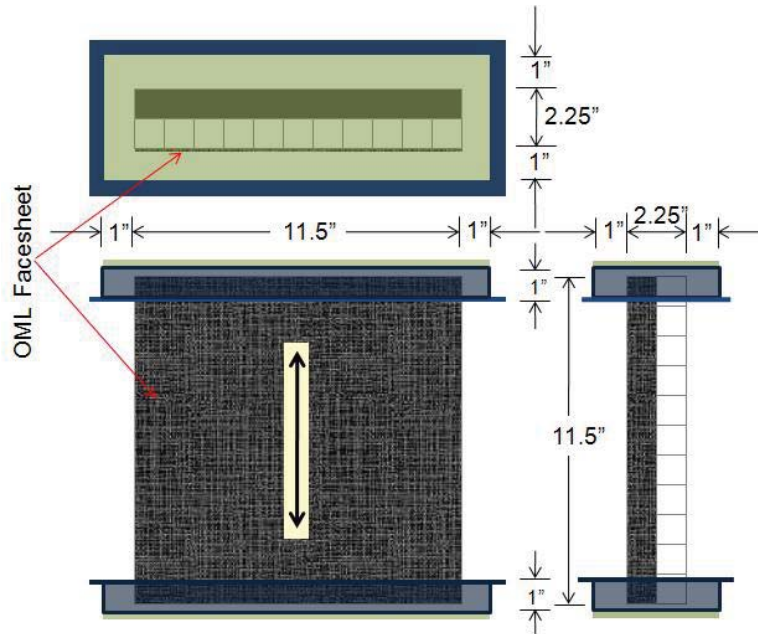


Figure 4. Requested Potting Geometry (Dimension in Inches)

The ends to be potted are designated by the arrow (\updownarrow) and were in the warp direction of the OML facesheet. Longitudinal AETB bars, running along OML facesheet, are in the loading direction. Transverse AETB bars, running along the IML facesheet, are perpendicular to the loading direction.

Note: The panel was embedded in the potting material $\sim 1/2$ inch at the top of the specimen and ~ 1 inch at the bottom. Although the specimen was not potted symmetrically on the top and bottom of the SITPS-0 panel, no detrimental effects were expected.

3.2. Specimen Instrumentation

The SITPS-0 panel was heavily instrumented with redundant systems due to the fact that only one panel existed and panel-level mechanical properties were of the utmost importance. The panel was instrumented with the following systems.

- DCDTs for out of plane displacements
- Strain gages for in-plane strains
- Photogrammetry for out of plane displacements
- Photogrammetry for in-plane strains
- Acoustic Emission sensors as a damage locator

The instrumented panel shown in the test load frame is presented in Figure 5.

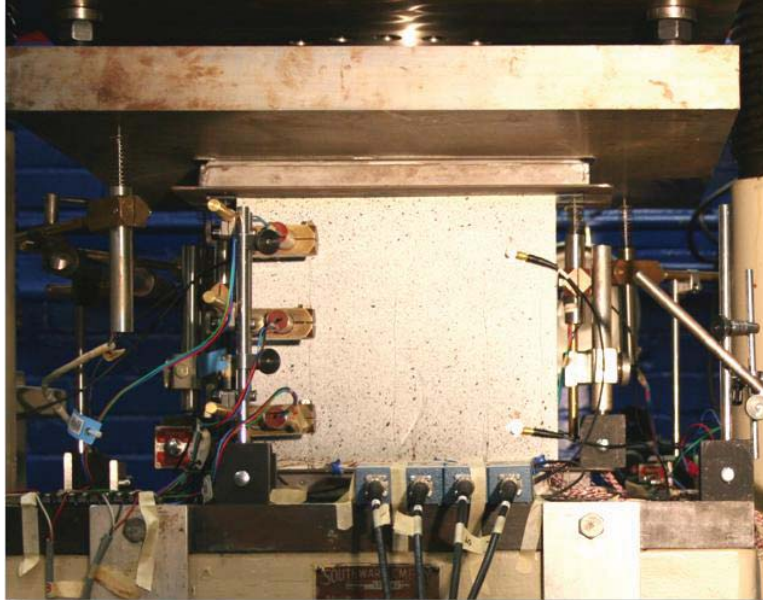


Figure 5. Instrumented SITPS-0 test article in test load frame (View of OML Facesheet)

The instrumentation layout on the OML and IML are identical as shown in the mirrored images in Figure 6. The vertical and horizontal lines indicate the 1-inch AETB bars to provide the instrumentation location relative to the AETB bars. The DCDTs (⊗) are located near the same edge of the specimen. A detailed discussion of each type of instrumentation is presented in the following subsections.



Figure 6. Instrumentation Layout

3.2.1. DCDTs (Out-of-Plane Displacements)

Three ± 0.25 -inch DCDTs (DC Displacement Transducers) (⊗) were placed perpendicular to the OML and IML to monitor specimen out-of-plane displacement

during loading and to distinguish between specimen bending deflections and facesheet disbonding. As shown in Figure 7, the DCDTs were placed roughly two inches from the left-hand side of the specimen (as viewed from the OML) and equidistant from the top of the specimen. The OML DCDTs were located at the intersection of AETB bars 2 and 3 (numbered left to right) and at the mid-span of AETB bars 3, 6 and 9 (numbered top to bottom) on the IML. The DCDT data was acquired at 10Hz (samples per second) using the Micro-Measurements Smart Strain (V3.10) data acquisition system and the Model 5100B scanners.

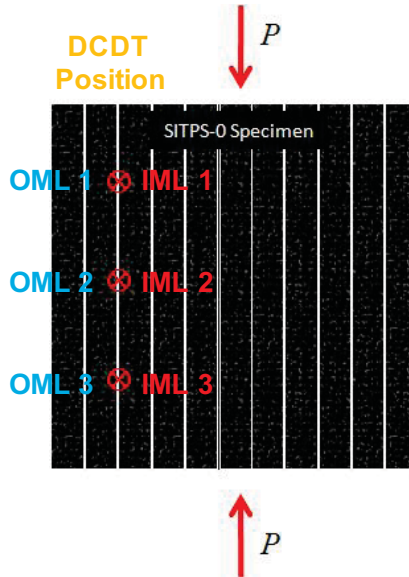


Figure 7. DCDT Layout for Bending and Out-of-Plane Displacements

3.2.2. Strain Gages (In-Plane Strain and Poisson's Ratio)

Twelve longitudinal strain gages (■) and one rectangular rosette strain gage (●) were installed on both the OML and IML facesheet at mid AETB bar locations as shown in Figure 8. The longitudinal strain gages are universal general purpose Measurements Group, Inc. CEA-06-187UW-350 (gage length = 0.187-inch) and the center strain gages are CEA-06-250UR-350 (gage length = 0.250-inch) placed in a rectangular rosette configuration (0°, 45° and 90°).

All strain gages were oriented for longitudinal strain with the exception of the center strain gages. The center strain gage are rectangular rosettes providing longitudinal and transverse strain to determine Poisson's effect under loading. The upper and lower corner strain gages on the OML and IML were used for platen alignment to ensure proper load introduction into the panel.

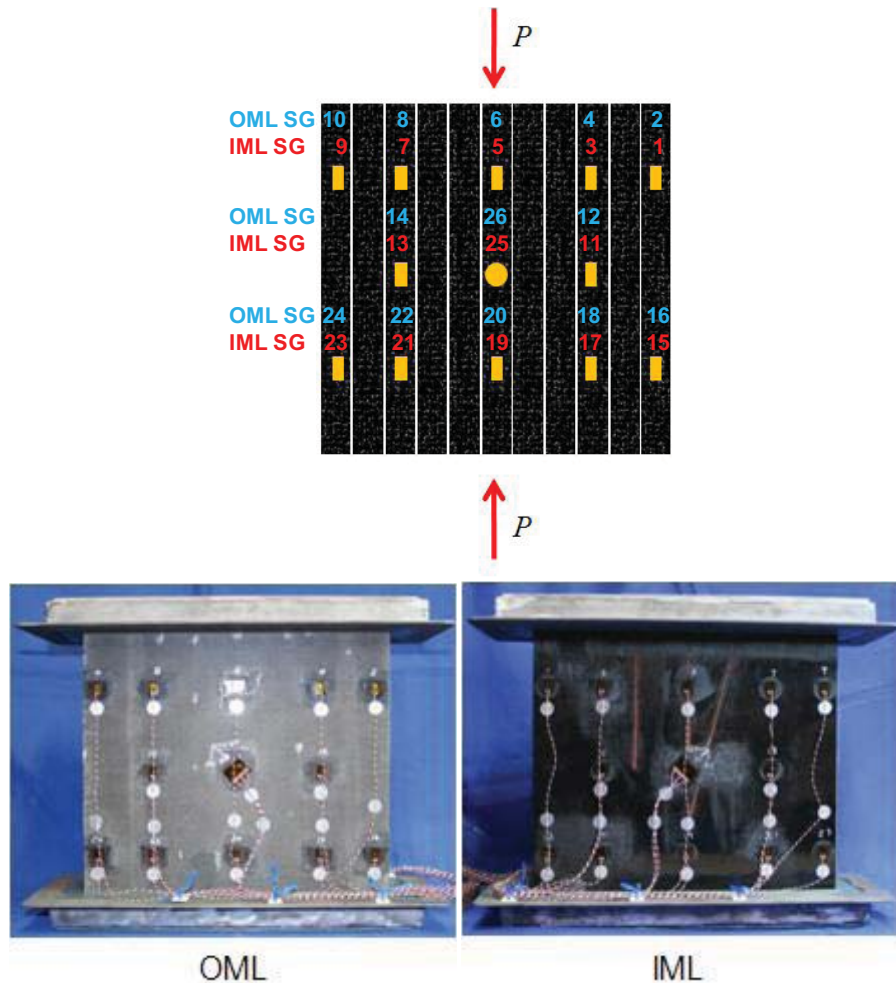


Figure 8. Strain Gage Locations for In-Plane Strains

The strain gage data was acquired at 10Hz using the Micro-Measurements Smart Strain (V3.10) data acquisition system and the Model 5100B scanners.

3.2.3. Photogrammetry (In-Plane Strain, Out-of-Plane Displacements)

Full field strain and out-of-plane deformations were monitored by photogrammetric methods using the VIC 3D (Video Image Correlation) System by Correlated Solutions, Inc. The VIC 3D System employs three-dimensional image correlation allowing the measurement of all three (X, Y and Z) surface displacement fields simultaneously. The OML and IML of the test article were spray-painted with white Krylon enamel paint and then sputtered with black Krylon enamel paint for use in the correlation algorithm.

The VIC 3D setup for the edgewise compression test of the SITPS-0 test article is shown in Figure 9. The setup consists of four 5-MByte monochrome cameras; two cameras each viewing the OML and IML simultaneously. The camera images were recorded at a rate of 2 frames per second. VIC 3D reports in-plane displacement with

accuracies up to 0.02 pixels and out-of-plane displacement accuracies up to 0.04 pixels; strain with accuracies up to 0.01% locally and 0.005% globally.

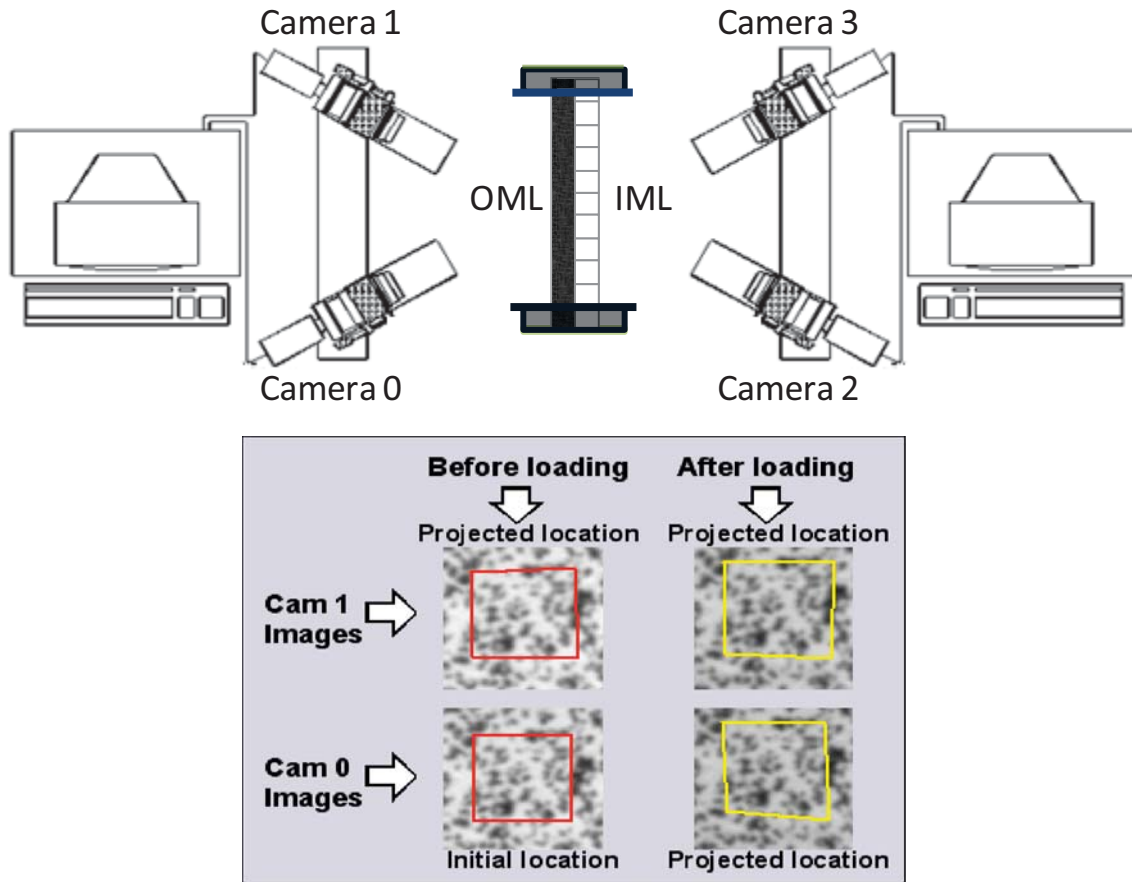


Figure 9. Photogrammetry System Setup

3.2.4. Acoustic Emission Sensors (Damage Indicator)

Four Acoustic Emission (AE) sensors (●) were mounted to the OML and IML facesheets (total of 8 sensors). The AE sensors monitor the AE activity (energy release from introduction of damage) in the specimen during loading. The locations of the AE sensors are shown in Figure 10 (as viewed from the OML).

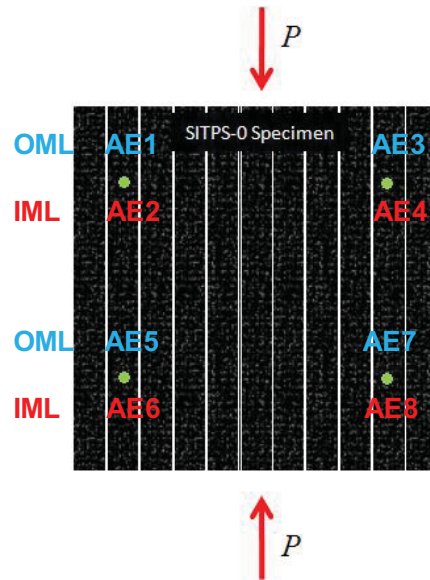


Figure 10. Acoustic Emission Sensor Location

The AE sensors were B1025 Sensors with a frequency bandwidth of 50 kHz - 2MHz. Tape was adhered to the specimen surface at the desired AE sensor location and the AE sensors were glued to the tape using an epoxy. The sensors were connected via the Digital Wave PA0 preamp/line to the Digital Wave FM1 signal conditioning 16 channel amplifiers. The AE activity was captured on a portable computer running the Wave Explorer software.

3.3. Test Stand

The test stand used was a 120-kip Southwark-Emery Test machine with a 6-inch maximum displacement (Figure 11). The test stand has a 23-inch x 24-inch leveling platen for maintaining proper load introduction. The leveling platen was instrumented with three additional ± 1.00 -inch DCDTs to monitor the trueness of the upper platen during the specimen loading. The platen DCDTs were placed equidistant (3-inch) from the platen edge. Platen alignment was accomplished using a pre-load on the specimen of 1000 lbs while monitoring strain gages at the corners of the specimen and adjusting the leveling screws on the platen until minimal strain deviation existed between the strain gages at the corners of the specimen.

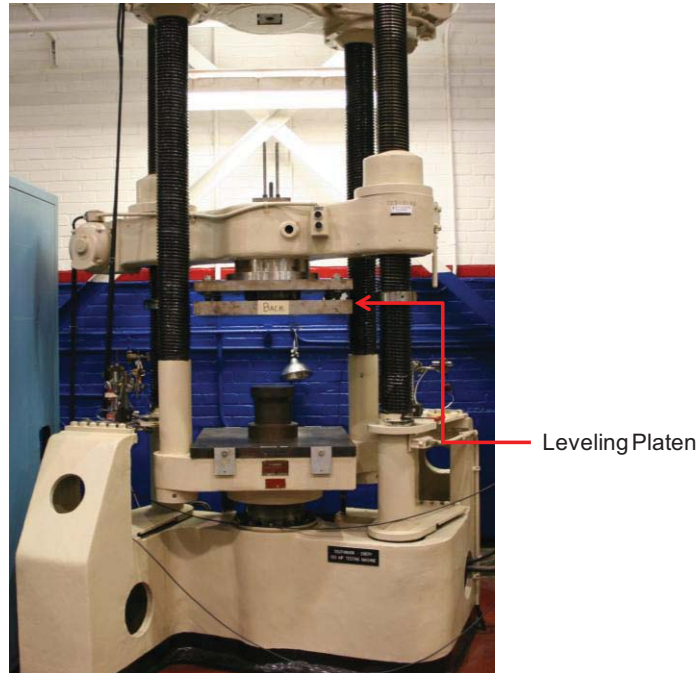


Figure 11. Southwark Emery 120-kip Test Stand

3.4. Test Sequence

The objective of the edgewise compression was to reach the proportional limit of the SITPS-0 panel in incremental loading steps. The proportional limit is considered to be the so-called first matrix cracking stress, i.e., the point where σ - ϵ curve becomes non-linear. The test sequence consisted of the three individual loadings listed in Table 1.

Table 1. Edgewise Compression Loading Sequence

Sequence	Target Load	Notes
1	10000 lbs (~390 psi)	<ul style="list-style-type: none"> • Zero all instrumentation prior to load introduction. • Acquire instrumentation data and photogrammetry.
2	20000 lbs (~780 psi)	<ul style="list-style-type: none"> • Do not re-zero instrumentation • Acquire instrumentation data and photogrammetry.
3	Proportional Limit	<ul style="list-style-type: none"> • Do not re-zero instrumentation. • Acquire instrumentation data and photogrammetry. Stop loading at proportional limit.

The SITPS-0 edgewise compression tests were run under displacement control at ~0.002 inches/min. Once the proportional limit was reached, the load was removed and

the specimen was inspected by NDE techniques – thermography and computed tomography.

4. TEST RESULTS

A summary of the results from the loading sequence of the edgewise compression test is shown in Table 2. A maximum of 37439 lbs (1459 psi) was attained at which time the loading was terminated. The proportional limit had been reached, and a suspected delamination was seen on the IML and bending was seen on the OML. The following subsections deals with the mechanical properties of the SITPS-0 panel loadings.

4.1. Compressive Elastic Modulus

The engineering stress, σ (psi) is defined as

$$\sigma = P/A \quad (1)$$

where P is the compressive load (lb) and A is the cross-sectional area ($A = 25.66 \text{ in}^2$).

The linear strain gages were used to monitor the strain in the specimen.

The computation of the elastic modulus was restricted to the linear portion of the σ - ε curve between $-100\mu\varepsilon$ and $-600\mu\varepsilon$ and ε was the average of SG 15 through 24. The elastic modulus, E (psi), is

$$E = \Delta\sigma / \Delta\varepsilon \quad (2)$$

where $\Delta\sigma/\Delta\varepsilon$ is the slope of the linear region of the σ - ε curve.

The compressive elastic moduli resulting from the three loadings are shown in Table 2 and graphically presented in Figure 12. Over the three loadings, a minor increase in modulus was seen. Moduli ranged from 1.095×10^{-6} to 1.146×10^{-6} psi.

Table 2. Compressive Elastic Modulus

Loading Sequence	Maximum Compressive Load (lbs) Stress(psi)	Line Load (lbs/in)	Compressive Strain ($\mu\epsilon$)	Compressive Elastic Modulus (psi)
10K	10094 lbs 432 psi	878 lbs/in	360 $\mu\epsilon$	1.095×10^6 psi
20K	20045 lbs 781 psi	1743 lbs/in	691 $\mu\epsilon$	1.128×10^6 psi
37K	37439 lbs 1459 psi	3256 lbs/in	1405 $\mu\epsilon$	1.146×10^6 psi

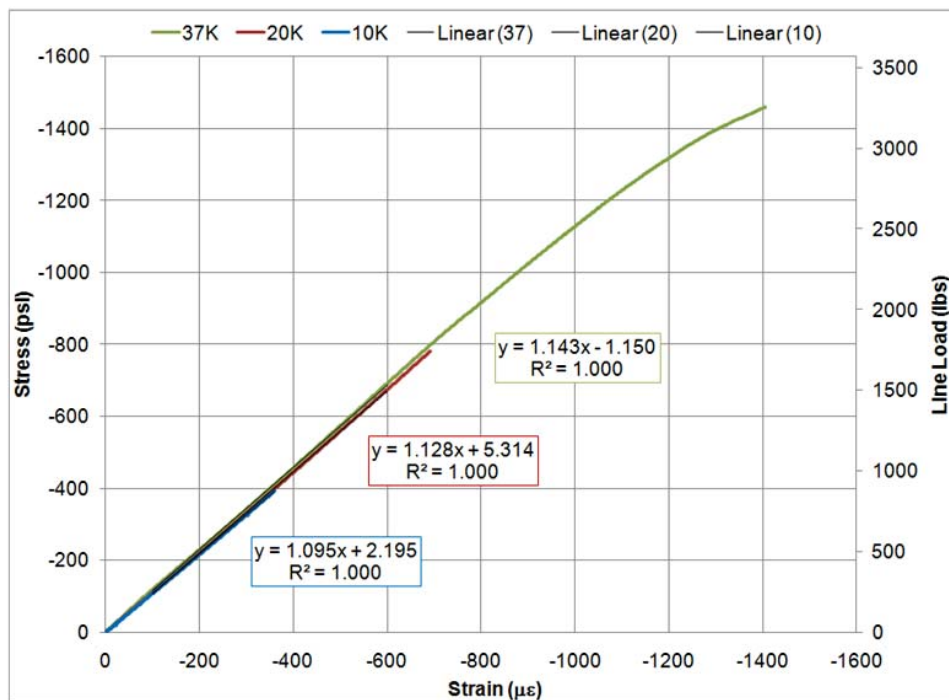


Figure 12. SITPS-0 Stress-Strain Curves (psi)

4.2. Proportional Limit

The proportional limit is determined using the offset method at a strain offset of $-5.0\mu\epsilon$. Using the elastic modulus (slope of the linear region of the σ - ϵ curve between $-100\mu\epsilon$ and $-600\mu\epsilon$ and the strain offset of $-5.0\mu\epsilon$, the offset line is drawn. The proportional limit (σ_{prop} and ϵ_{prop}) is the point at which the offset line intersects the σ - ϵ curve. The proportional limit occurred at $\sigma_{prop} = 1039$ psi at a $\epsilon_{prop} = -914\mu\epsilon$ corresponding to a total load of 26671 lbs and a line load of 2319 lbs/in. The graphical representation is shown in Figure 13.

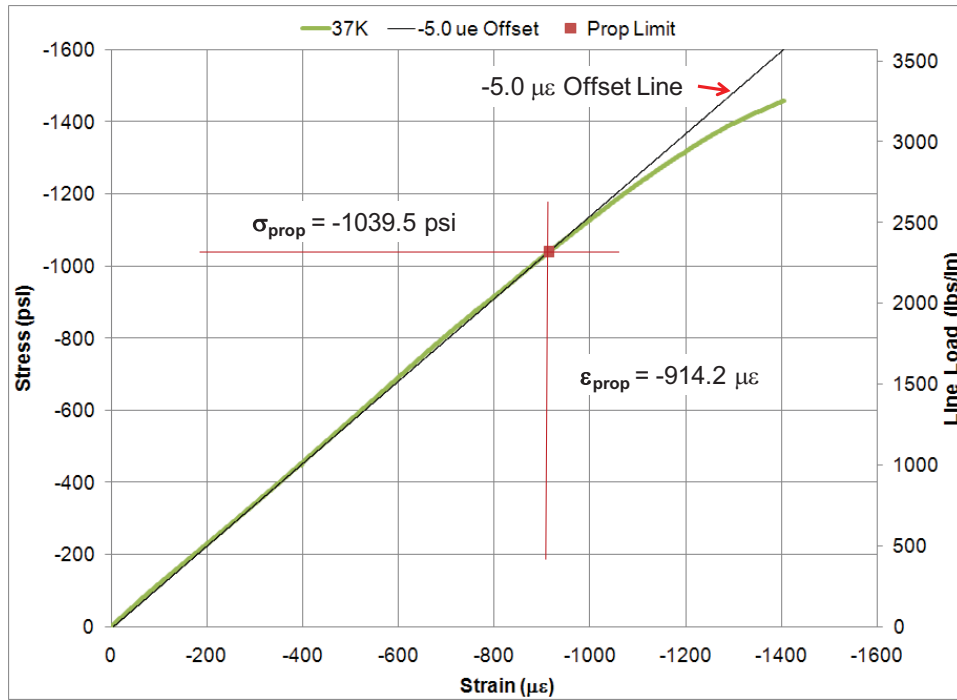


Figure 13. SITPS-0 Proportional Limit (Offset = -5.0 $\mu\epsilon$)

4.3. Poisson's Ratio

Poisson's ratio, ν , for each facesheet (OML and IML) was determined using the data from the rectangular rosette strain gages at the center of the specimen on each of the facesheets. Poisson's ratio uses the slope of the linear region of the ϵ_T - ϵ_L curve

$$\nu = \Delta\epsilon_T / \Delta\epsilon_L \quad (3)$$

$\Delta\epsilon_T/\Delta\epsilon_L$ is the slope of the linear region of the ϵ_T - ϵ_L curve where ϵ_T is the transverse strain and ϵ_L is the longitudinal strain.

The transverse vs. longitudinal strain for each loading is presented in Figure 14.

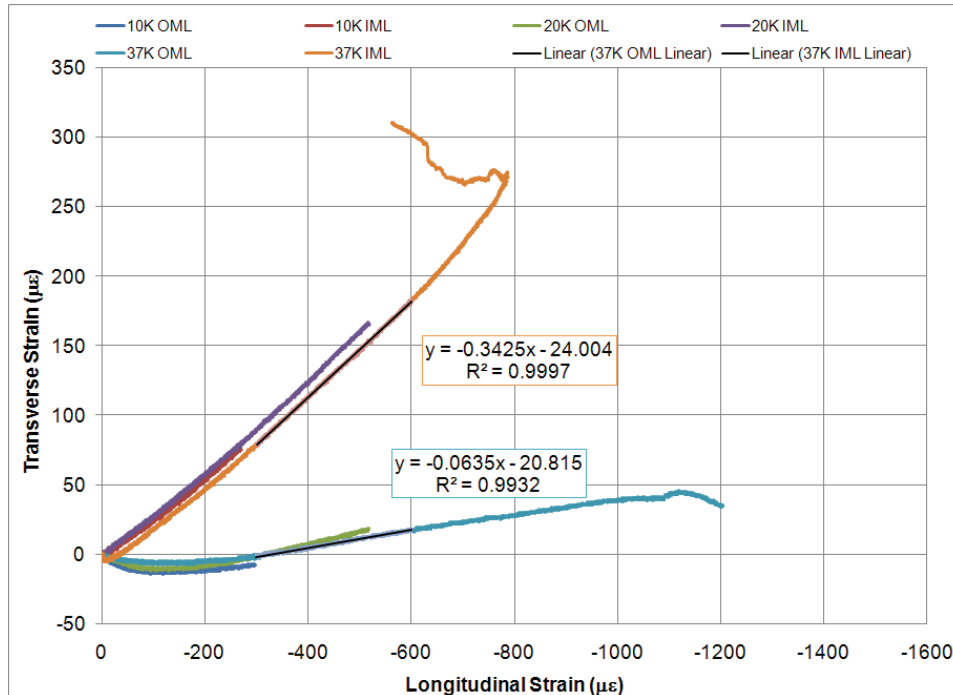


Figure 14. Rosette strain gage response used to calculate Poisson's ratio for each Facesheet

Poisson's ratio (37K loading) was determined as the slope of the linear portion of the 37K lbs loading step occurring at longitudinal strains between -300 and $-600\mu\epsilon$. Poisson's ratio for the OML and IML is presented in Table 3.

Table 3. Poisson's Ratio

Facesheet	Poisson's Ratio, ν (37K)
OML (S200Hm)	0.064
IML (M55J/954-3)	0.343

4.4. Bending / Out-of-Plane Displacements

The DCDTs, Photogrammetry System, and the AE sensors were monitored for bending and out-of-plane displacements. See Specimen Instrumentation (Section 3.3) for the locations of the instrumentation.

4.4.1. DCDTs

A total of six DCDTs were positioned perpendicular to the OML and IML facesheets (three DCDTs on each facesheet) during the loading sequence. The sign convention for the DCDT displacement data is shown in Figure 15. A positive displacement on the IML

facesheet indicates an outward displacement away from the centerline of the specimen. A negative displacement on the OML facesheet indicates an outward displacement away from the centerline. The converse is true in both cases.

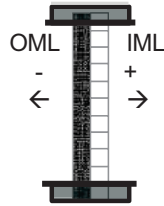


Figure 15. DCDT Out-of-Plane Displacement Sign Convention

The DCDT displacements resulting from the three loading sequences are shown in Figures 16 – 18. It should be emphasized that the data presented in the following figures represent the panel response where the DCDT are located.

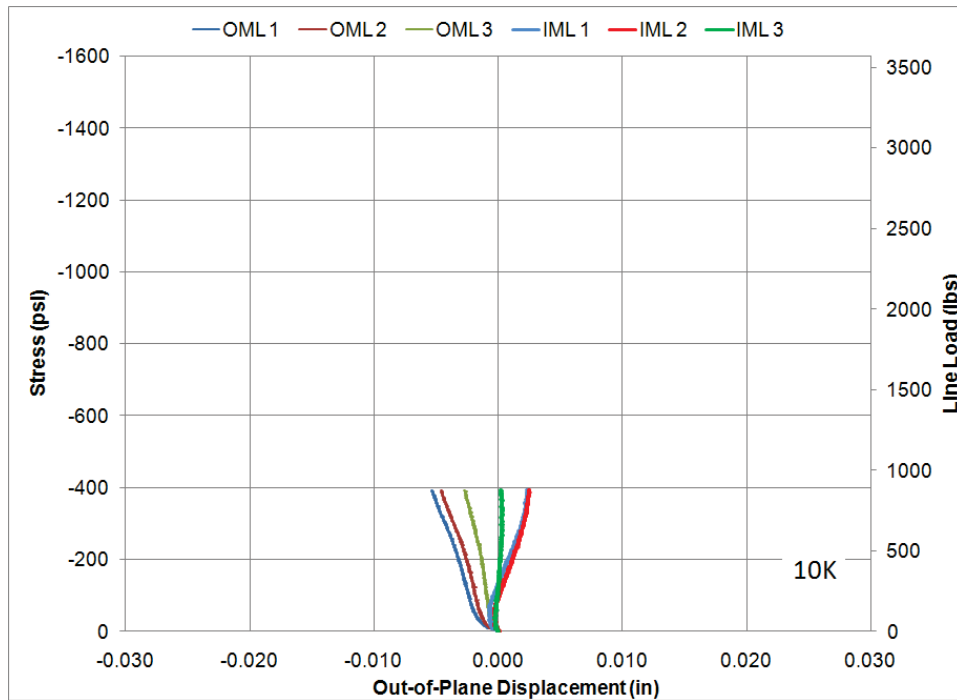


Figure 16. Out-of-Plane Displacement (DCDT) - 10K Loading Sequence

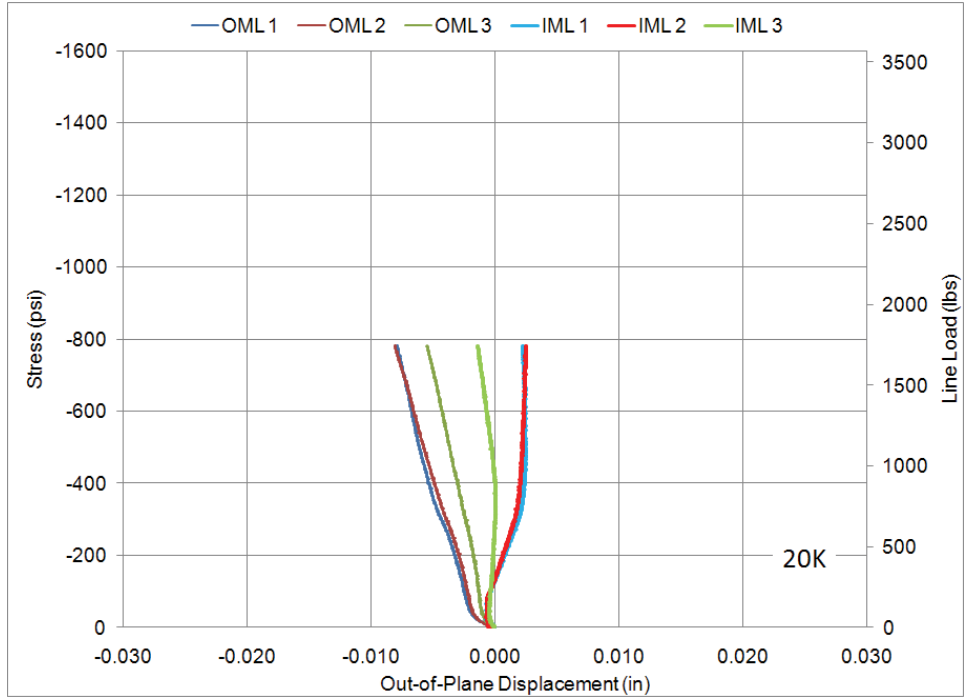


Figure 17. Out-of-Plane Displacement (DCDT) - 20K Loading Sequence

The displacements for the 10K and 20K loading sequence indicates the initiation of bending of the OML beginning at the onset of loading. The displacements on the OML are somewhat larger than the IML.

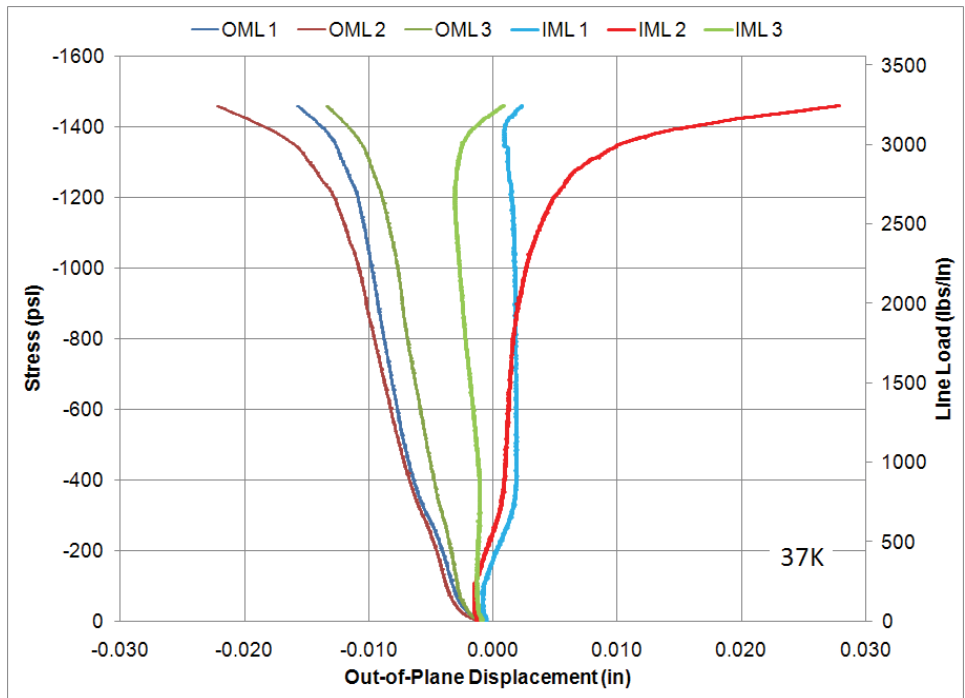


Figure 18. Out-of-Plane Displacements (DCDT) - 37K Loading Sequence

The DCDT displacements resulting from the 37K loading sequence are shown in Figure 18. The OML displacements show a somewhat symmetrical bending about the centerline of the specimen. The displacement at the center of the specimen (OML 2) has the largest out-of-plane displacement with respect to the upper (OML 1) and lower (OML 3) DCDTs. OML1 and 3 exhibit somewhat similar behavior although differ in magnitude.

The displacements for the IML indicate a much different behavior. The upper (IML 1) and lower (IML 3) DCDTs remain somewhat stable whereas the behavior at the center of the IML (IML 2) shows a divergence from IML1 and 3 starting at 800 psi. At 1000 to 1200 psi, IML 2 shows a very rapid increase in out-of-plane displacement indicating a delamination of the facesheet.

A rough depiction of the out-of-plane displacement at the DCDT locations shown in the Figure 19 illustrating the bending of the OML facesheet and delamination on the IML.

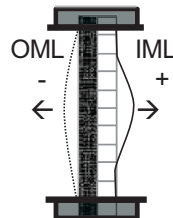


Figure 19. Overview of Out-of-Plane Displacements @ 37K lbs

4.4.2. Photogrammetry

The photogrammetry data provides a global view of the panel response. The photogrammetric results from the VIC System Z-Displacement output (out-of-plane displacements) for the OML and IML at 37K lbs load are shown in the Figure 20. The photogrammetry images do not contain the full field image due to obstruction of DCDTs, strain gage wires and AE instrumentation. Also note that the accuracy of out-of-plane displacements was sacrificed for accuracy of full field strain measurements. The center of the specimen is marked with rectangular strain gage (•).

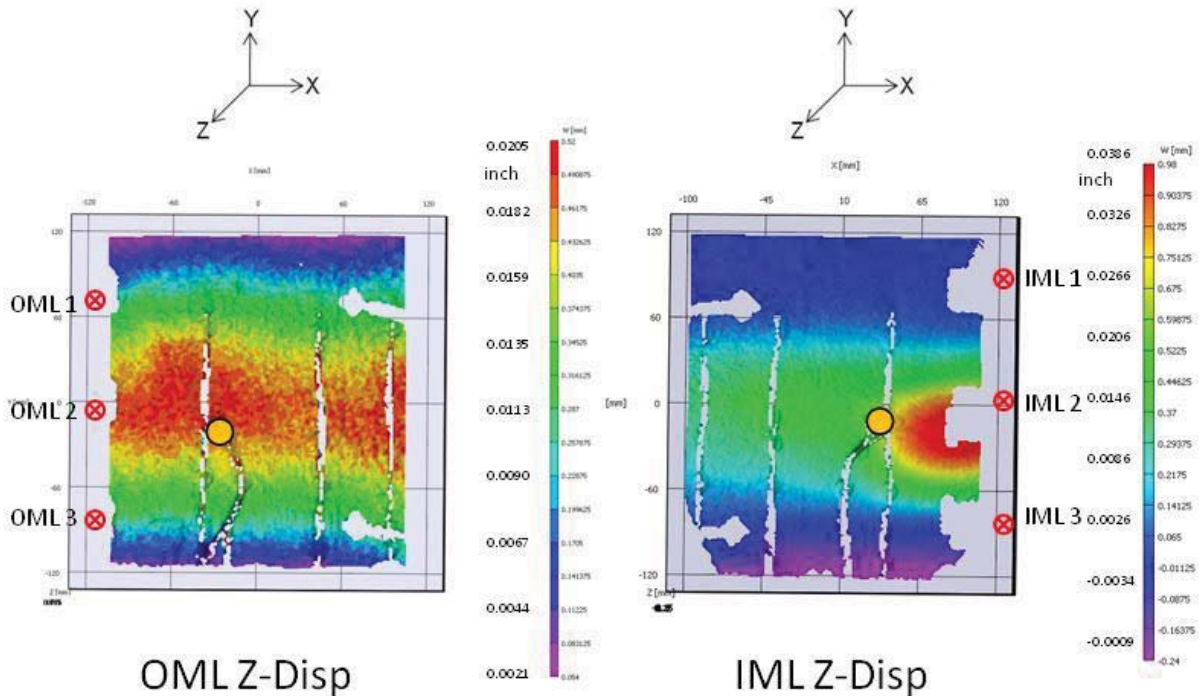


Figure 20. Out-of-Plane Displacements at P = 37K lbs (Photogrammetry System)

The Z-Displacements recorded by the photogrammetry system indicate bending on the OML as shown by the symmetrical lateral bands about the center of the specimen. The highest Z-Displacement occurs about the center of the specimen with lower Z-Displacement occurring at the top and bottom of the specimen. The photogrammetry data corresponds well to the out-of-plane displacement recorded by the DCDTs.

The Z-Displacements recorded on the photogrammetry system indicates slight bending of the IML with a pronounced Z-Displacement occurring near the location of DCDT IML2 which indicative of a delamination. The photogrammetry data corresponds well to the out-of-plane displacement and delamination recorded by the DCDTs.

A loading history (37K σ - ϵ curve) and the photogrammetry system images for out-of-plane displacements on the IML is shown in Appendix A. No evidence of the delamination on the IML was apparent in the first two loading sequences. The delamination initiated at approximately 1000 psi of the third loading sequence followed by a rapid increase in out-of-plane displacement as supported by the SITPS-0 instrumentation.

4.4.3. Acoustic Emission

The Acoustic Emission (AE) sensors were installed on the OML and IML facesheets to monitor the energy release associated with the introduction of damage. See Specimen Instrumentation (Section 3.3) for the locations of the AE sensors. The AE

data were filtered to remove low amplitude events (threshold = 50 mV) and only includes events that were received by at least two sensors.

The AE activity for the 37K loading is shown in Figure 21. The histogram of First Occurrence Arrival indicates which sensor first detected an AE event.

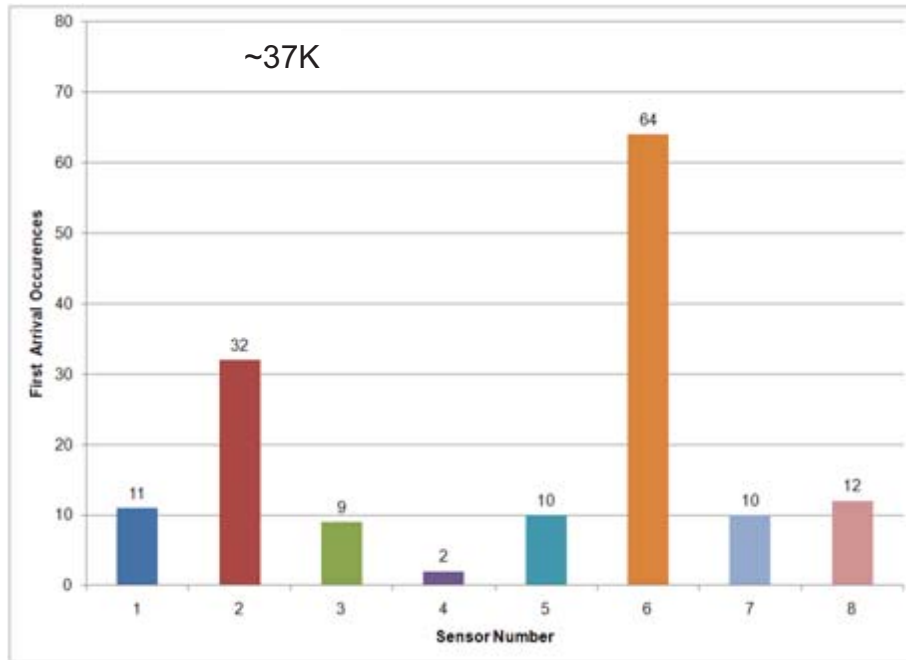


Figure 21. Acoustic Emission - First Arrival Occurrences

The odd-numbered AE sensors, located on the OML, show an even distribution of first arrival occurrences. However, the even numbers sensors, located on the IML, show a disparity in the distribution of first arrival occurrences with AE6 and AE2 having the greatest number of first arrival occurrences whereas AE 4 and AE8 have much fewer occurrences. Hence, the majority of AE activity was occurring in the region of sensors AE6 and AE2 on the IML.

The AE activity on the IML also corroborates the expected delamination shown by the out-of-plane displacements from the DCDT data, strain gage data and photogrammetry Z-Disp images on the IML.

4.5. In-Plane Strains

4.5.1. Longitudinal Strain Gages

The strain gage output for the OML and IML from the 37K loading sequence is shown in Figure 22 (See Figure 8 for the locations of the strain gages). OML strains were fairly linear throughout the 37K loading whereas the IML strains were non-linear.

SG 11, 13 and 25 were located at the site of the expected delamination and showed a deviation from the linear response starting at ~1000 psi. The behavior of SG 11, 13 and 25 are a classic behavior for delamination.

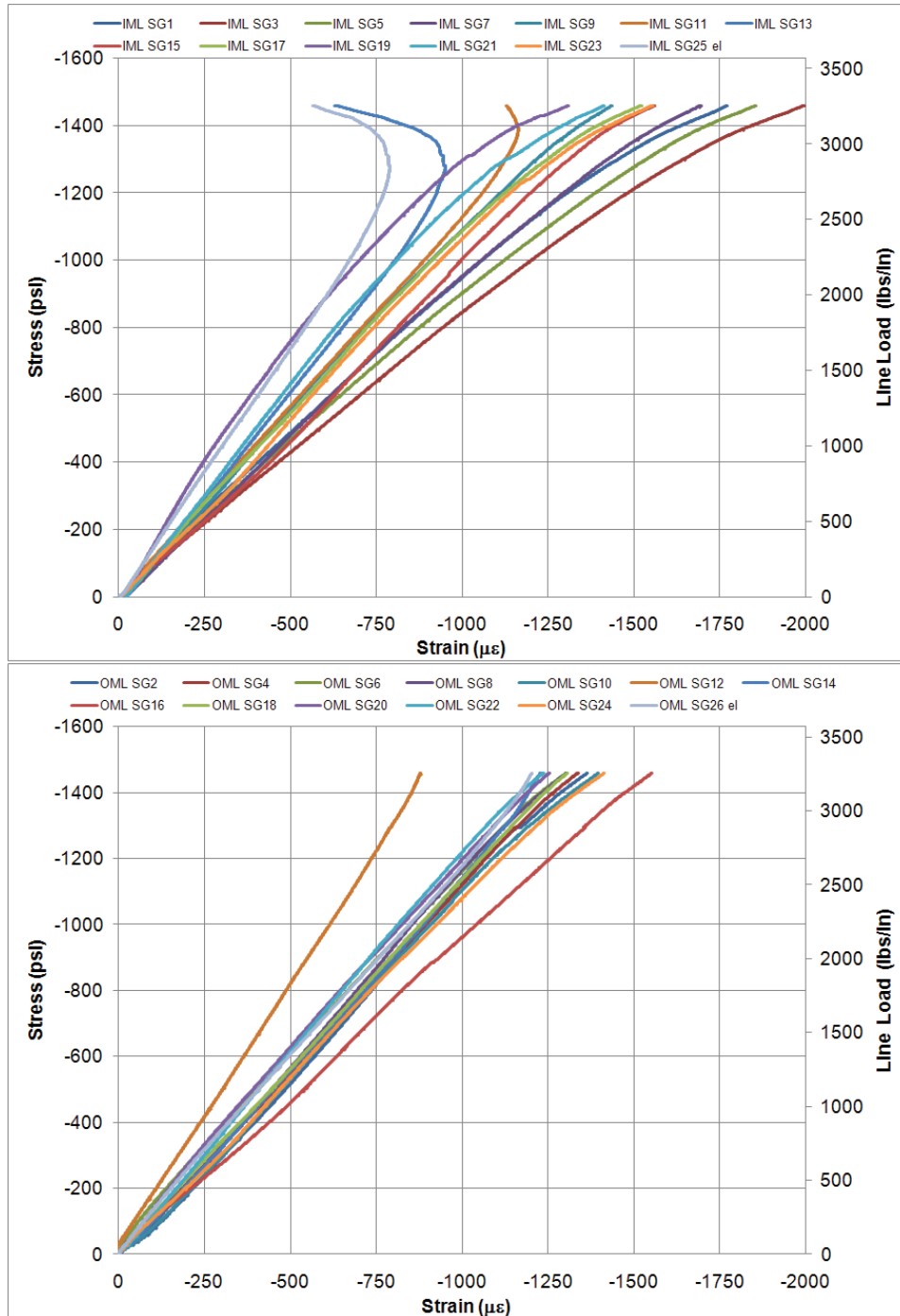


Figure 22. In-Plane Strains (Strain Gage Data)

4.5.2. Photogrammetry

The magnitude of the in-plane strains as reported by the photogrammetry system correlate reasonably well with the in-plane strains from the strain gage data reported in the previous section. The in-plane strains (ϵ_{yy}) from the photogrammetry system near the end of the test are shown in Figure 23. The high strain region on the right-hand side of the IML also indicates a delamination of the IML facesheet.

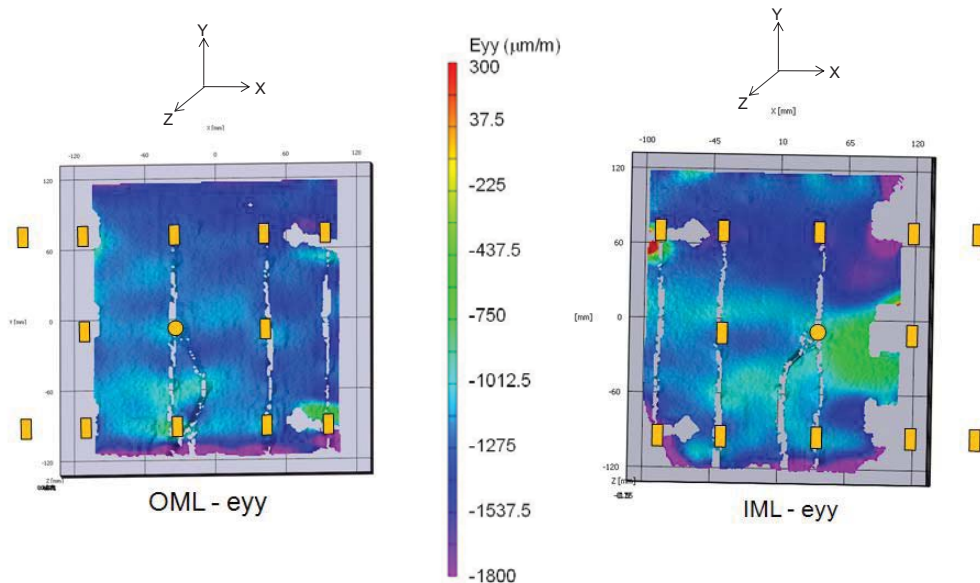


Figure 23. In-Plane Strains at P = 37K lbs (Photogrammetry System)

4.6. Post-Test Non-Destructive Evaluation

4.6.1. Thermography Image of Delamination

As a follow-up to the delamination issue as indicated by the out-of-plane displacements (DCDT and photogrammetry system), the in-plane strains (strain gages and photogrammetry system) and the AE activity, a post-test thermography image was taken of the IML of the unloaded SITPS-0 panel. The IML of the specimen was coated with GE Aerocoat-C spray prior to thermography inspection to increase the emissivity of the surface image and the thermography viewing was extended to two minutes. The thermography image (Figure 24) confirms the delamination on the right-hand side of the IML and is indicated by the light to white region of the image.

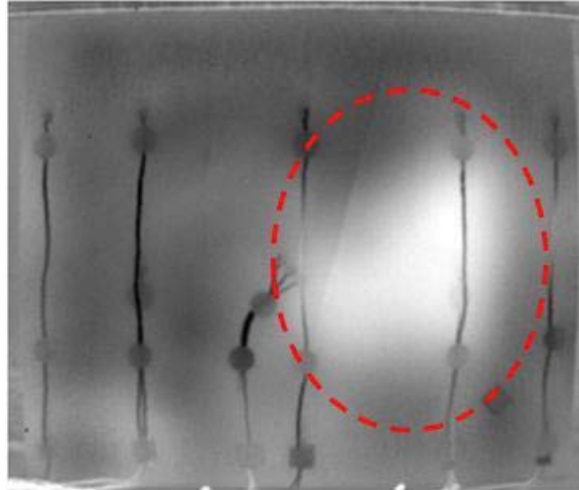


Figure 24. Thermography Image of IML showing delamination indicated by region within the dashed oval

4.6.2. Computed Tomography (CT)

Computed Tomography (CT) images were taken of the SITPS-0 specimen prior to and after the edgewise compression test for damage inspection. In both sessions, the CT images were taken under no load. It was assumed that the out-of-plane deformations on the OML and IML may have caused damage to the SITPS-0 specimen.

Damage could include fiber fracture, matrix cracking, fiber breakage, etc. on the OML and fracture of the IML. However, no damage was apparent in the CT images when comparing pre- and post-test CT images. Figure 25 shows the viewing aspect and highlights the constituents and thermocouple insertion points in the SITPS-0 panel. See Appendix B for additional post-test CT images.

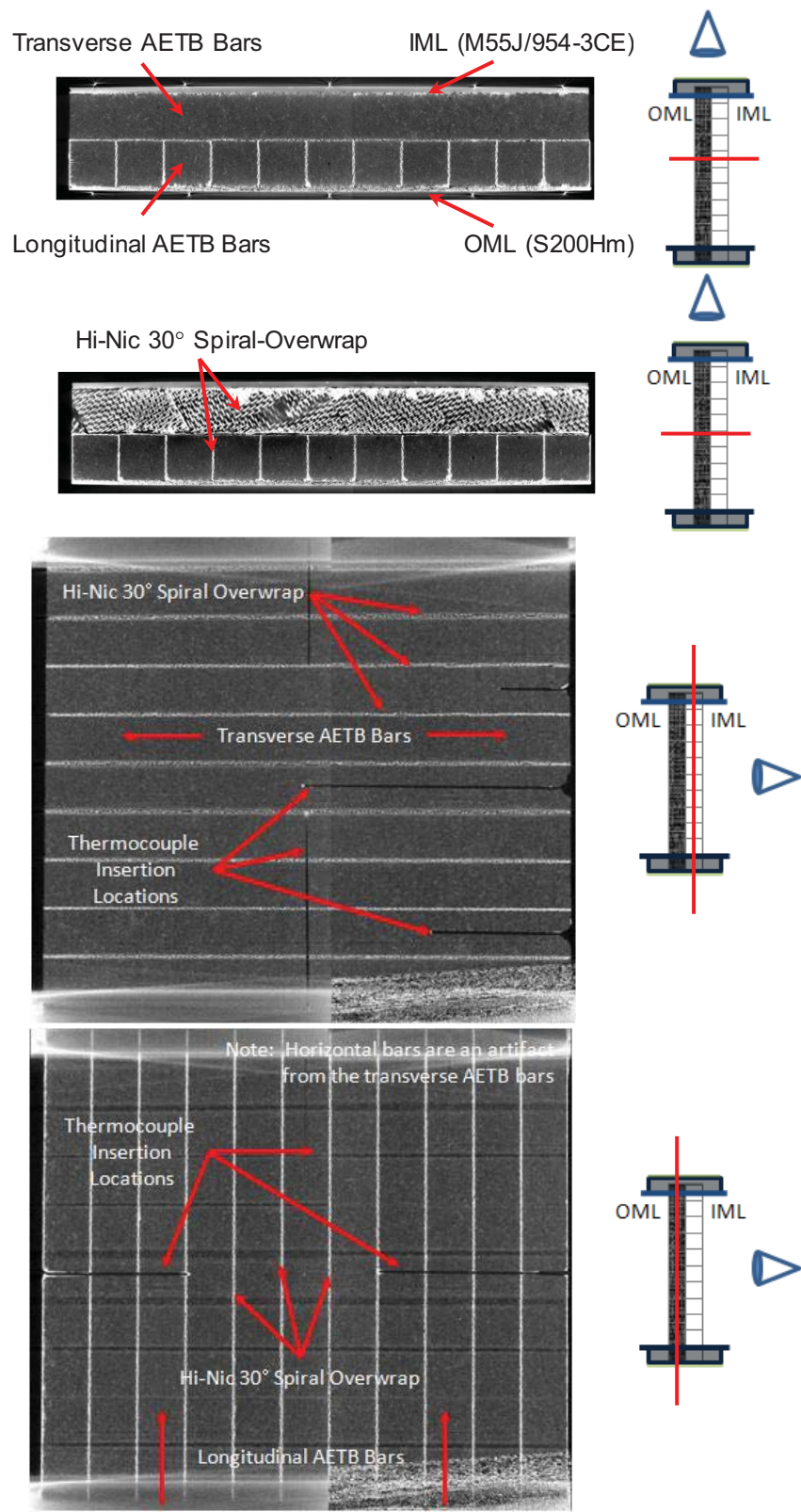


Figure 25. Post-Test CT Images

5. CONCLUSIONS

The Structurally Integrated Thermal Protection System (SITPS), was initiated under the NASA Hypersonics Program to develop a structural load-carrying thermal protection system for use in aerospace applications. The SITPS panel consists of high-temperature composite facesheets and a light-weight insulation structural core.

An edgewise compression test at room temperature was performed on the SITPS-0 specimen in order to obtain mechanical properties and behavior of the panel. The specimen was fully instrumented for out-plane displacements (DCDTs and photogrammetry) and in-plane strains (strain gages and photogrammetry) in addition to test frame load.

The specimen was potted and loaded such that the OML (S200Hm facesheet) was in contact with the longitudinal AETB bars and the IML (M55J/954-3 facesheet) was in contact with the transverse AETB bars. The SITPS-0 test article was subjected to a sequence of loadings; 393 psi (Load = 10090 lbs, Line Load = 877 lbs/in), 781 psi (Load = 20045 lbs, Line Load = 1743 lbs/in) and 1459 psi (Load = 37439 lbs (Line Load = 3256 lbs/in).

The compressive elastic modulus was determined to be $E = 1.146 \times 10^6$. The proportional limit was determined using a $-5.0 \mu\epsilon$ offset at $\sigma_{prop} = 1039$ psi (Load = 26671 lbs, Line Load = 2319 lbs/in) @ $\epsilon_{prop} = -914.2 \mu\epsilon$. Poisson's ratio (37K loading) was calculated to be $\nu_{OML} = 0.064$ and $\nu_{IML} = 0.343$.

Out-of-plane displacements (DCDTs and photogrammetry) indicated bending of OML and bending/partial delamination on the IML which resulted in a barrel-shape displacement about the center of and at the edge of the specimen. The AE First Arrival Occurrences also indicated high activity on the IML at the location of the suspected delamination. The delamination of the IML was corroborated with Thermography inspection.

OML strains were linear during loading whereas the IML strain were non-linear throughout the loading. There was reasonable correlation between in-plane strain (ϵ_{yy}) and the photogrammetry system.

The SITPS-0 specimen incurred bending of the OML and delamination of the IML under lower than expected loads. Further compression testing of the panel would not yield additional information such as ultimate load and strain.

Investigations of the SITPS-0 test article will continue to assess and confirm the actual size and location of the IML delamination, i.e., IML/glue layer, glue/overwrap layer, overwrap/AETB separation, etc. Also, the material properties of the individual

constituents of the as-built test article are being investigated and are required to aid in the development of the analytical models predictions for future testing.

REFERENCES

1. Easler, Tim; Plunkett, Rich; “Structurally Integrated Thermal Protection System”, Presented at National Space & Missile Materials Symposium, Henderson NV, 24 June 2009.
2. Darybeigi, Kamran; Knutson, Jeffrey; Martin, Kim, “Thermal Testing for Validation of Thermal Modeling of Structurally Integrated Thermal Protection System”, Presented at the 34th Annual Conference on Composites, Materials and Structures, Cocoa Beach FL, January 25-28, 2010.
3. Standard Test Method for Monotonic Compressive Strength Testing of Continuous Fiber-Reinforced Advanced Ceramics with Solid Rectangular Cross-section Test Specimens at Ambient Temperatures”, ASTM C1358-05.

APPENDIX A: IML OUT-OF-PLANE DISPLACEMENTS (Photogrammetry)

The following images show the loading history (loading to 37K lbs (maximum load occurs at Frame 866) and unloading) and the out-of-plane displacement photogrammetry images of the IML facesheet. The photogrammetry frame numbers are indicated on the σ - ϵ curve shown in Figure A-1. The photogrammetry images do not contain the full field image due to obstruction of DCDTs, strain gage wires and AE instrumentation. The accuracy of out-of-plane displacements was sacrificed for accuracy of full field strain measurements. The delamination emanates from the right side of the IML (Frame 600) and travels inwards toward the center of the specimen. The delamination was confirmed by Thermography. Overall, the IML facesheet experienced bending.

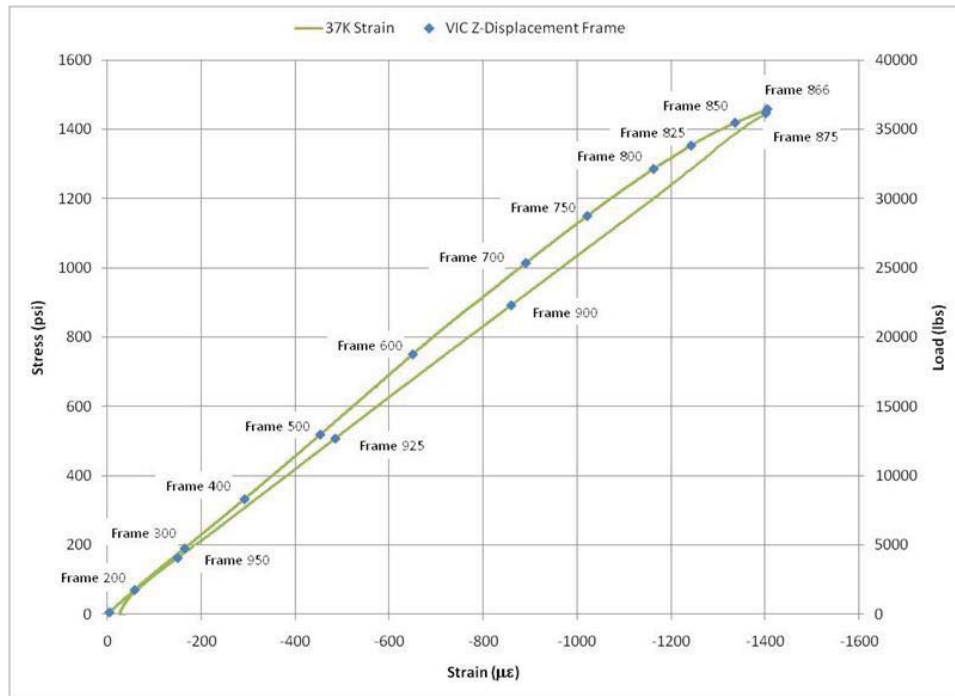


Figure A-1: Photogrammetry Image (Frame) with respect to Stress-Strain Curve

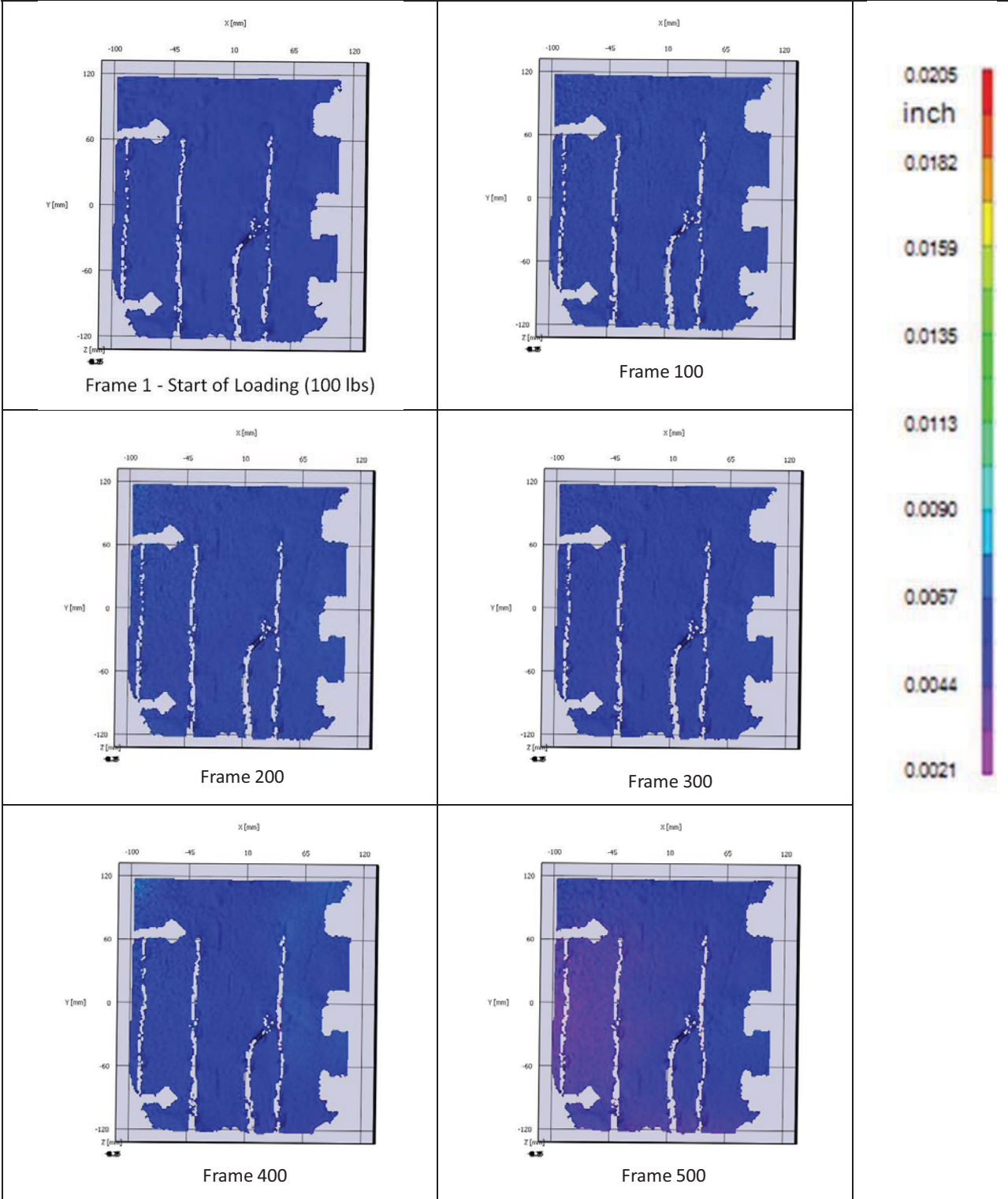


Figure A-2. Photogrammetry Images

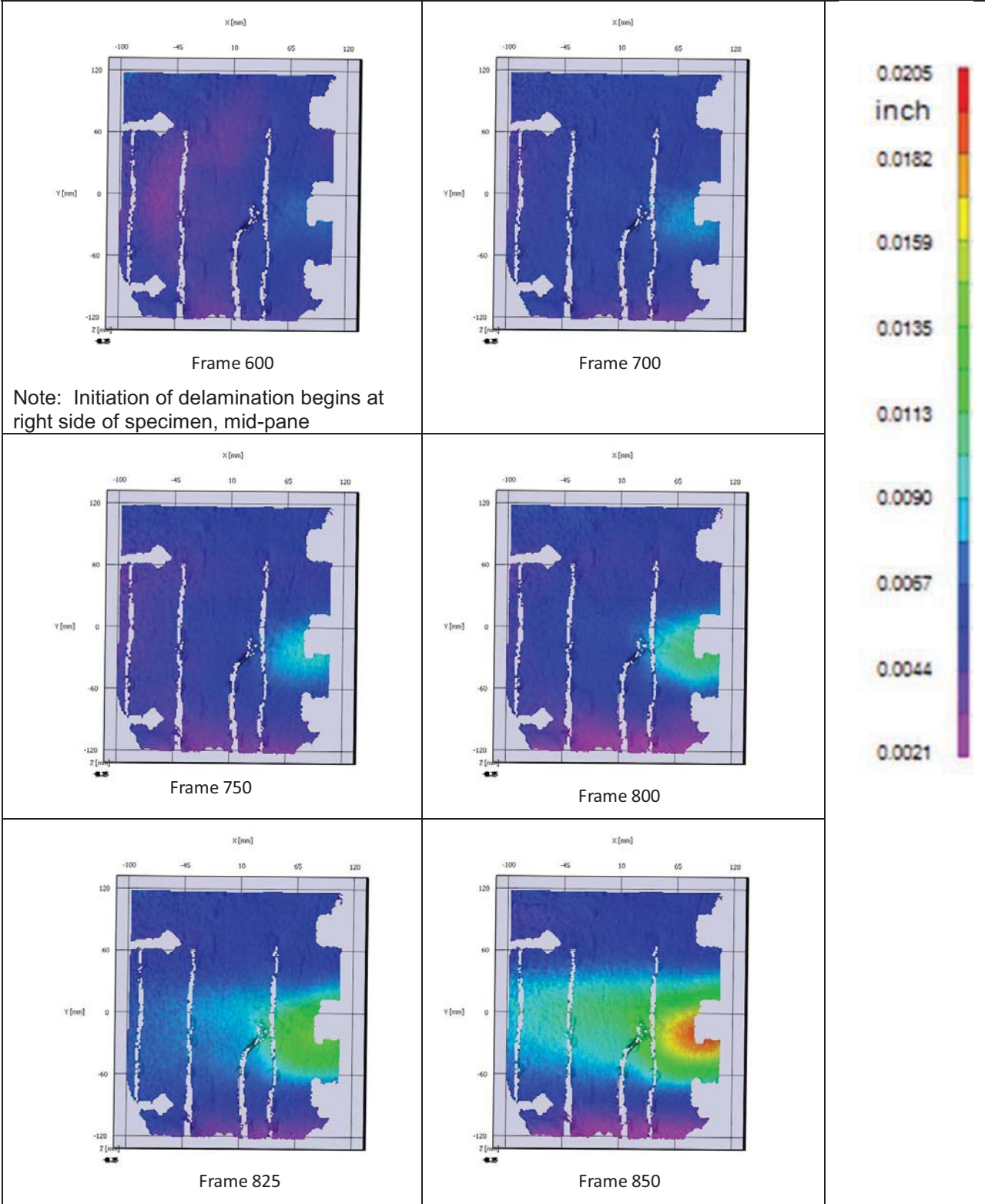


Figure A-3. Photogrammetry Images (continued)

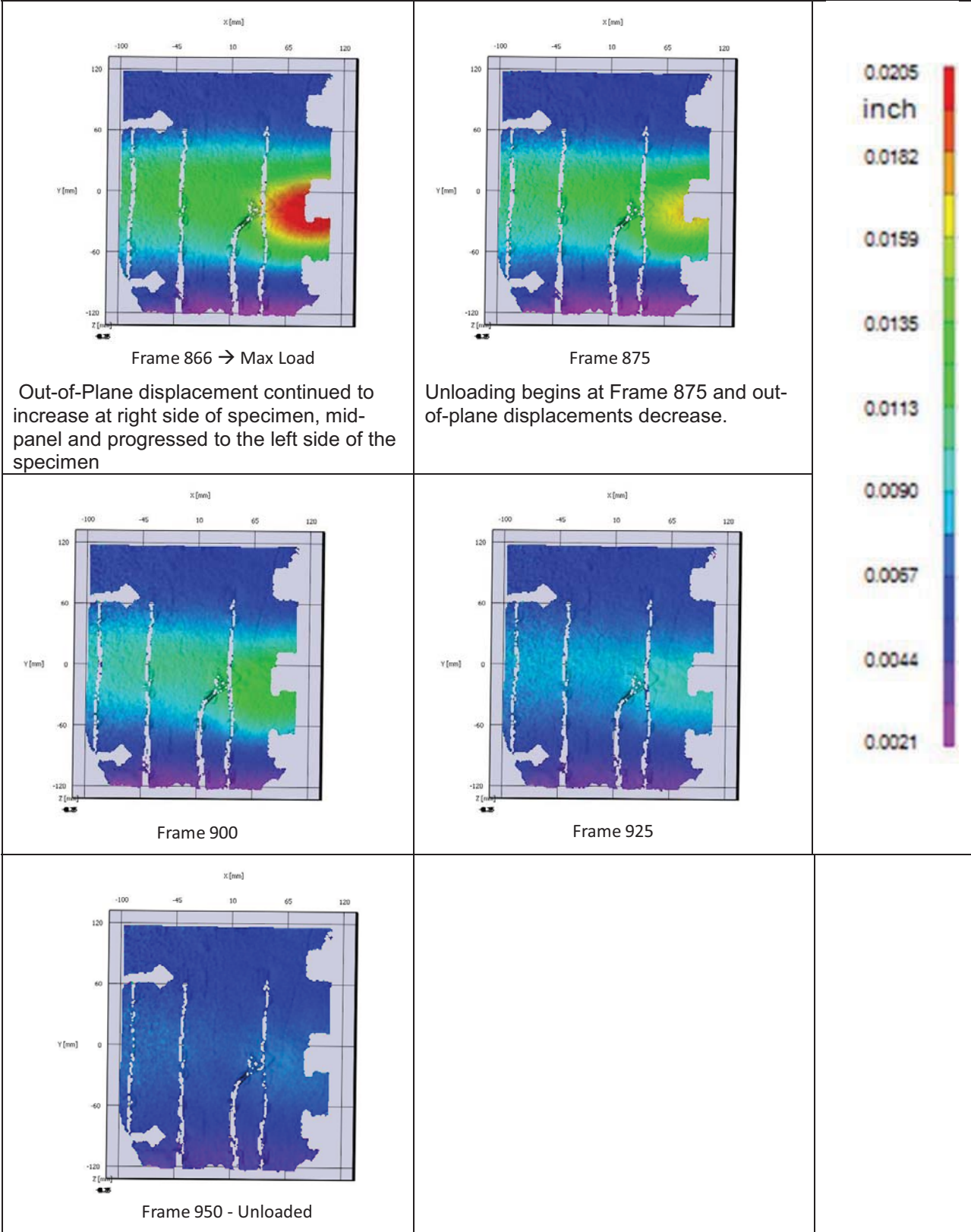


Figure A-4. Photogrammetry Images (continued)

APPENDIX B: Post-Test CT IMAGES

Computed Tomography (CT) images were taken of the SITPS-0 panel after completion of the edgewise compression testing. The following images are taken under no load. The images were taken in quadrants and comparisons should be limited to within the quadrant. In general, the density can be related to the pixel intensity in the images; lower density is darker, higher density is lighter to white.

The CT images are viewed from the IML facesheet to the OML and are denoted as Through Thickness. Next, images as viewed from the top of the specimen to the bottom of the specimen and are denoted as Through Depth. The viewing orientations are shown below and the location of the image is marked by the red line on the specimen layout, the frame number of each image is shown to mark the progression of CT images through the specimen.

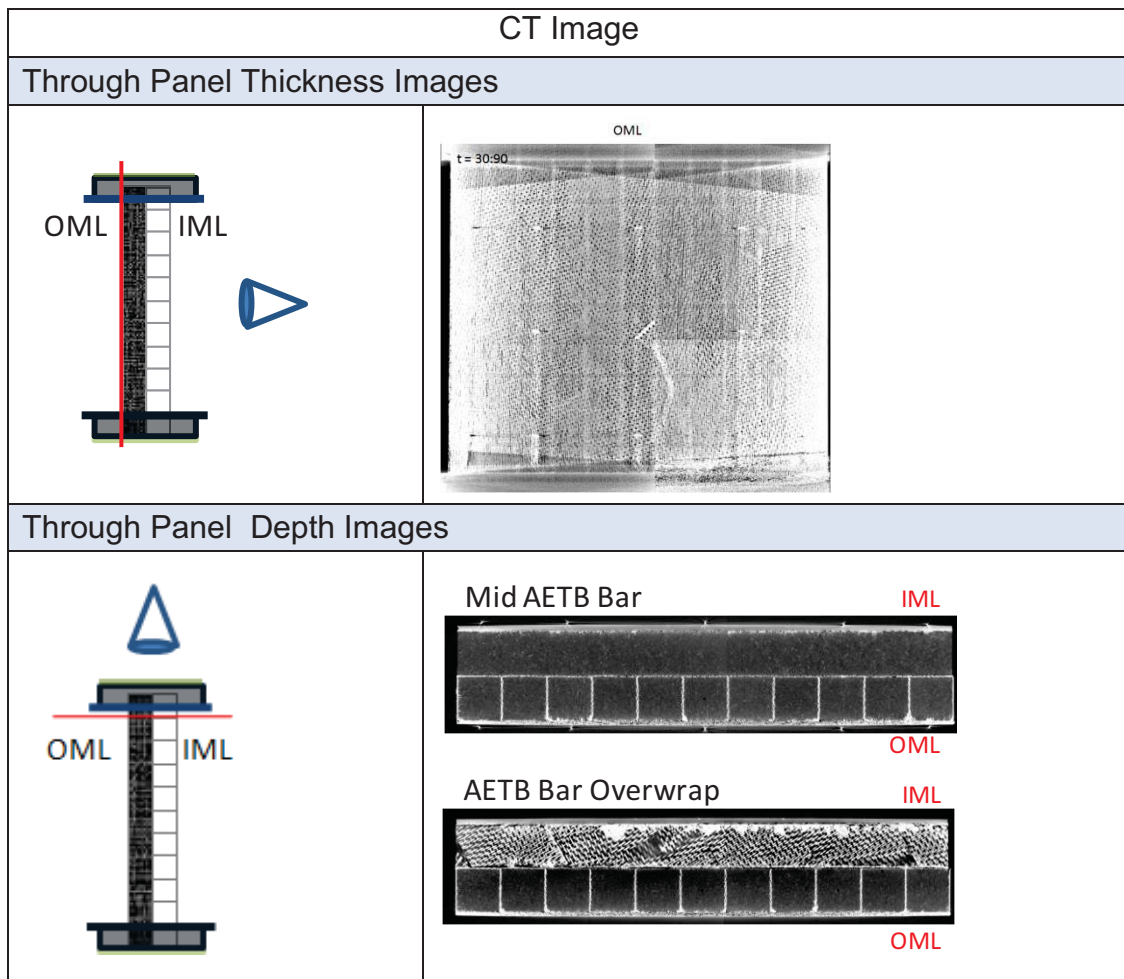


Figure B-1. Viewing Orientation for CT Images

B.1 Voids at Overwrap Intersections

Voids at the intersection of the AETB overwrap were prevalent throughout the SITPS-0 panel. These voids are interstitial spaces and are not to be confused with cracks. The voids were present prior to and after both the thermal cycling and the edgewise compression testing.

Examples of voids follow in Figure B-2.

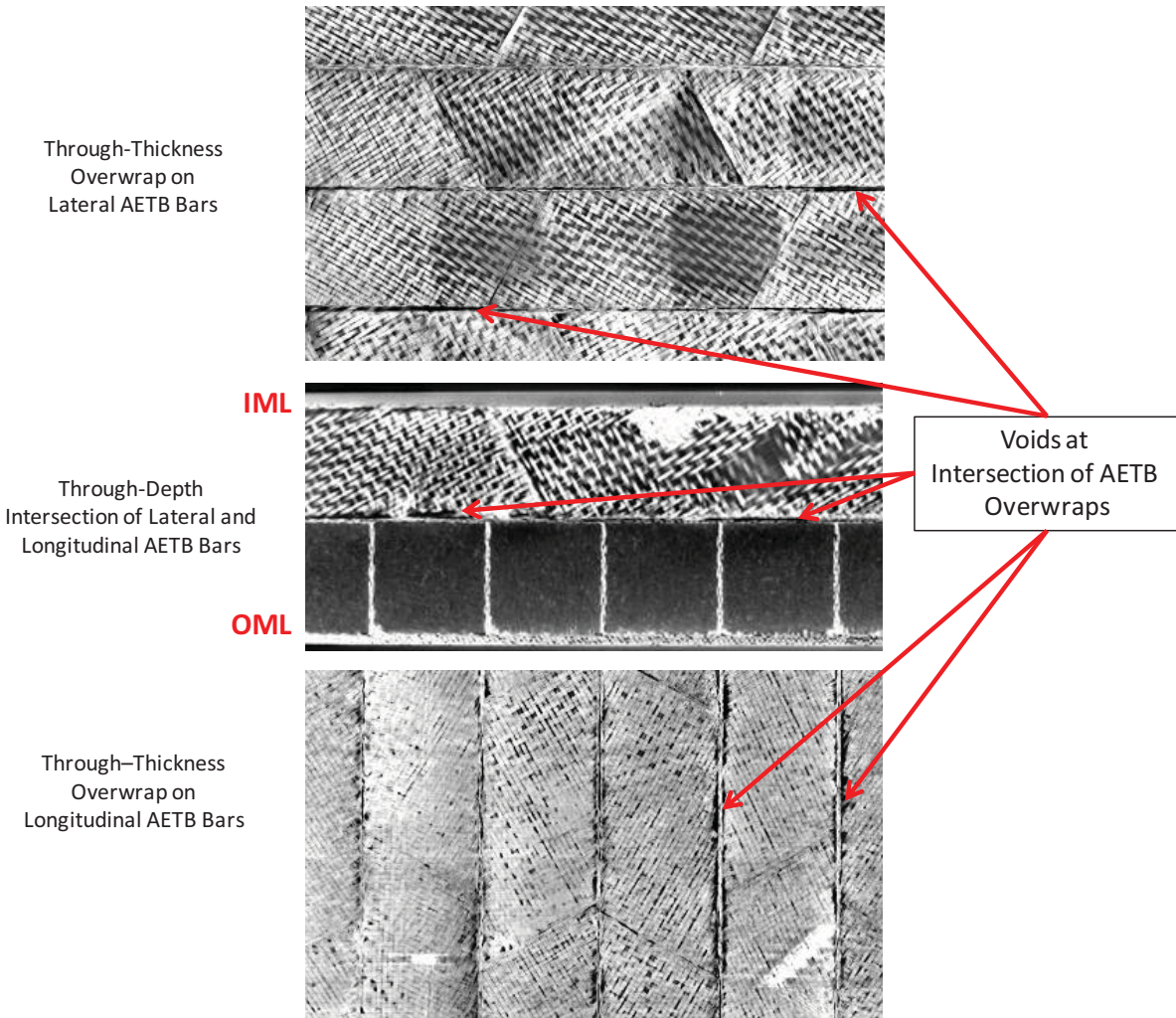


Figure B-2. Voids at AETB Overwrap Intersections

B.2 Through Panel Thickness - CT Images of SITPS-0

Note: Distortion at the top and bottom of the images are due to interference with the potting frame. The through-panel thickness CT images are shown in Figure B-3.

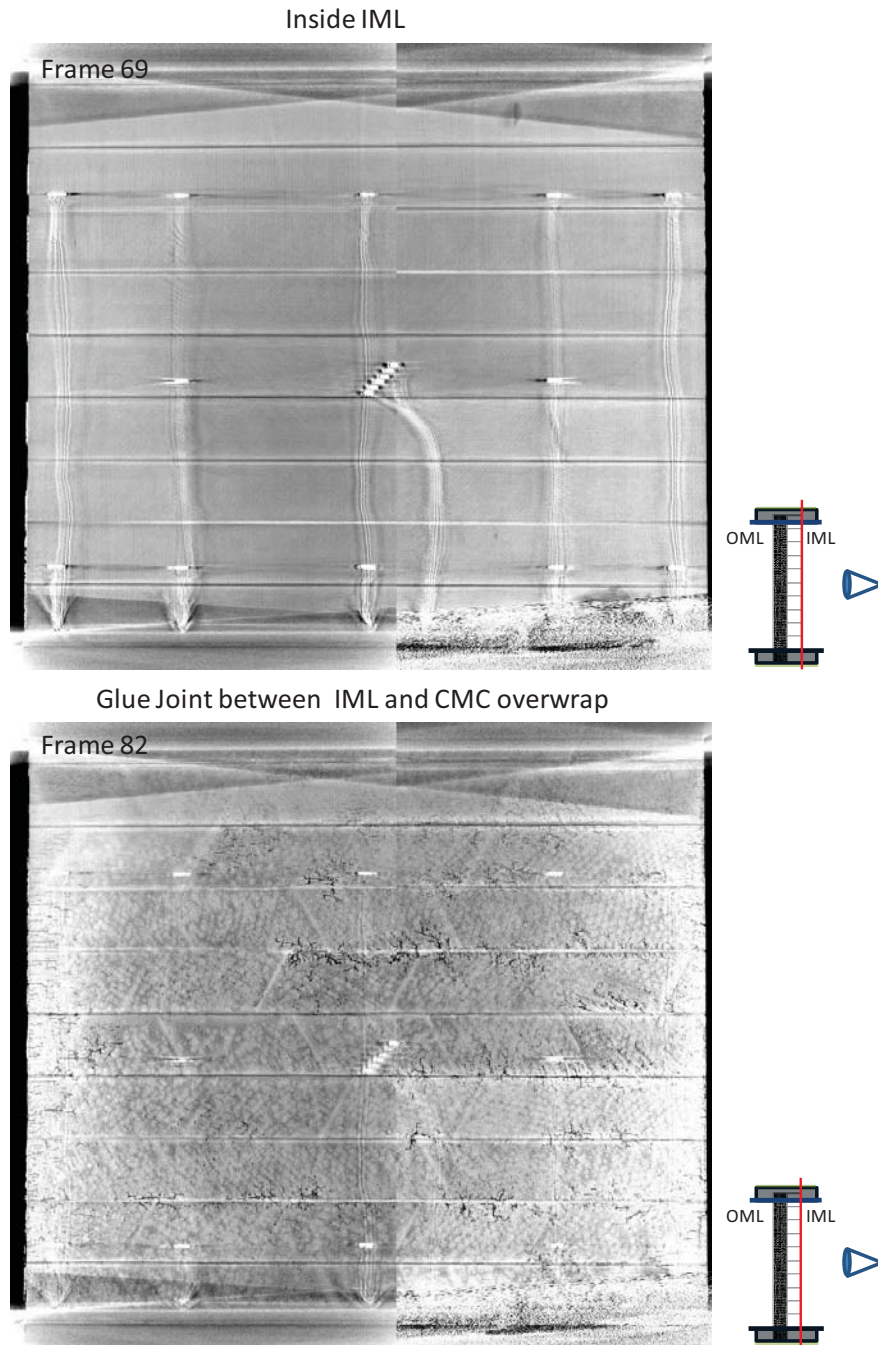
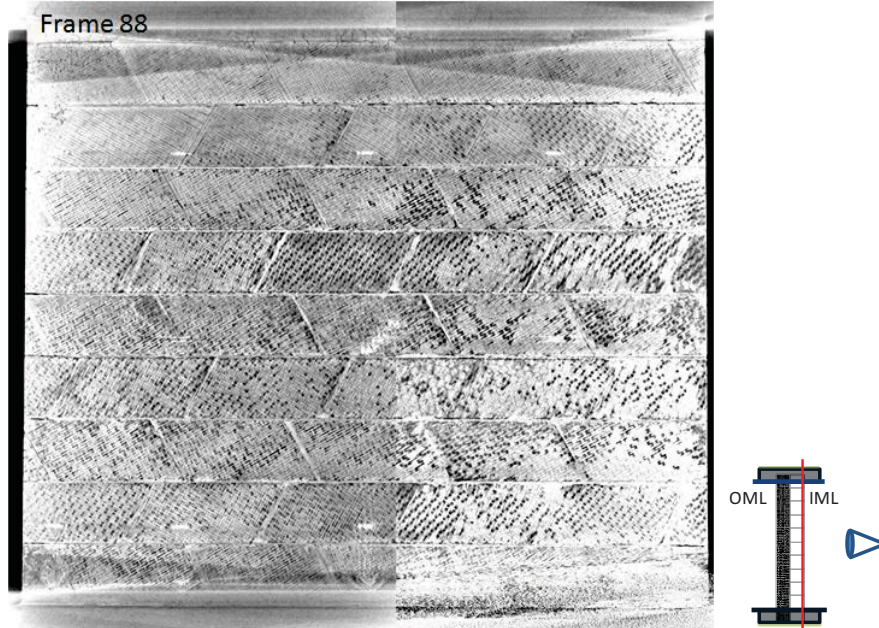


Figure B-3. Through Panel Thickness - CT Images of SITPS-0

Overwrap on transverse AETB bars



Partial View of Panel

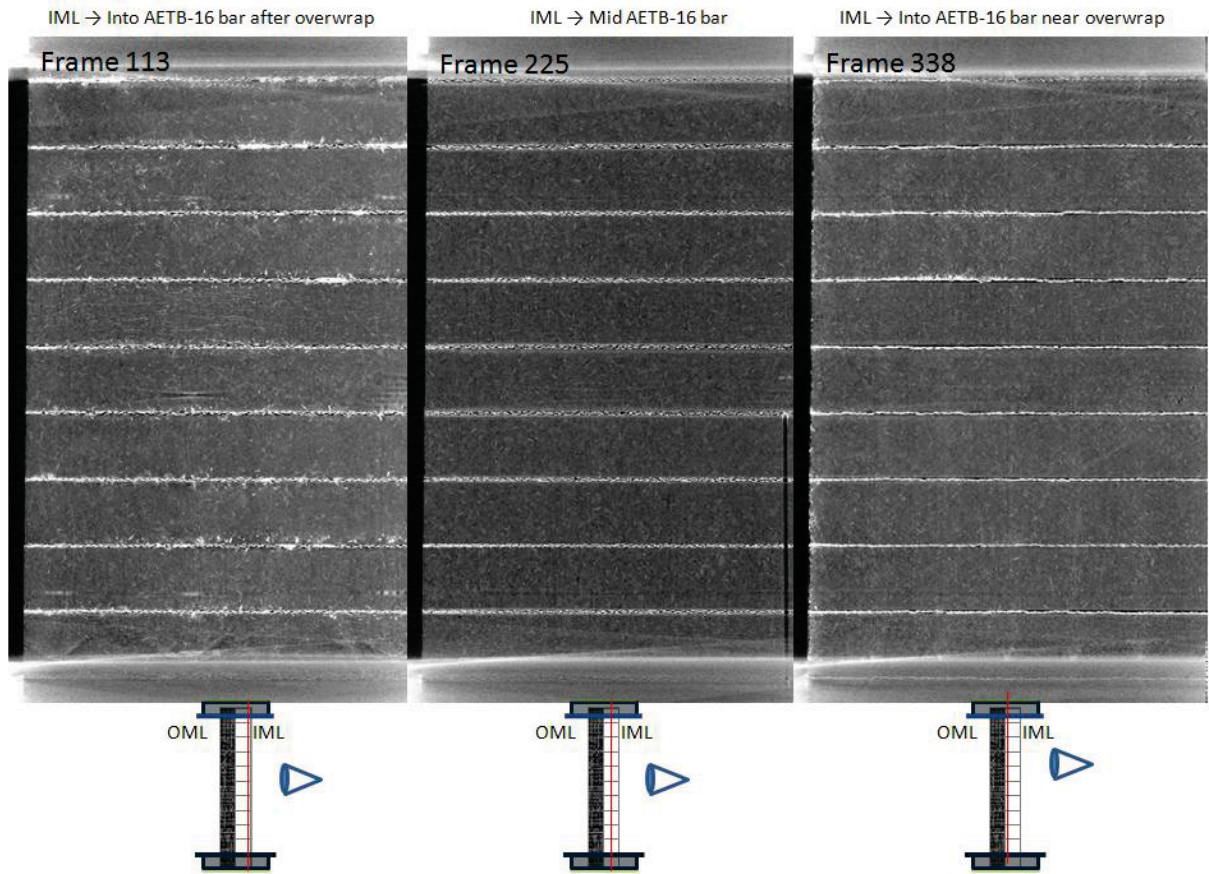
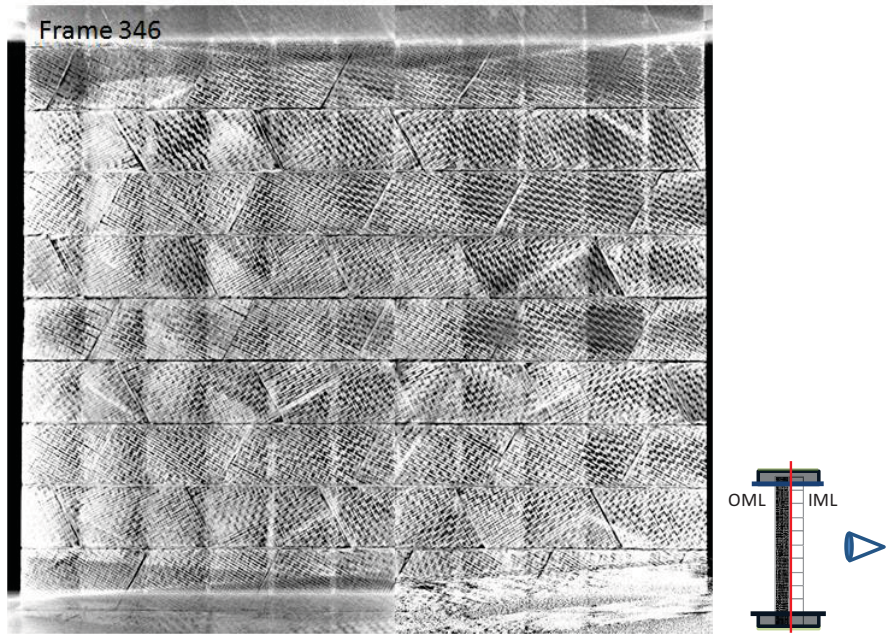


Figure B-3. Through Panel Thickness - CT Images of SITPS-0 (continued)

Overwrap on transverse AETB-16 bars at CL



Overwrap on longitudinal AETB-16 bars at CL

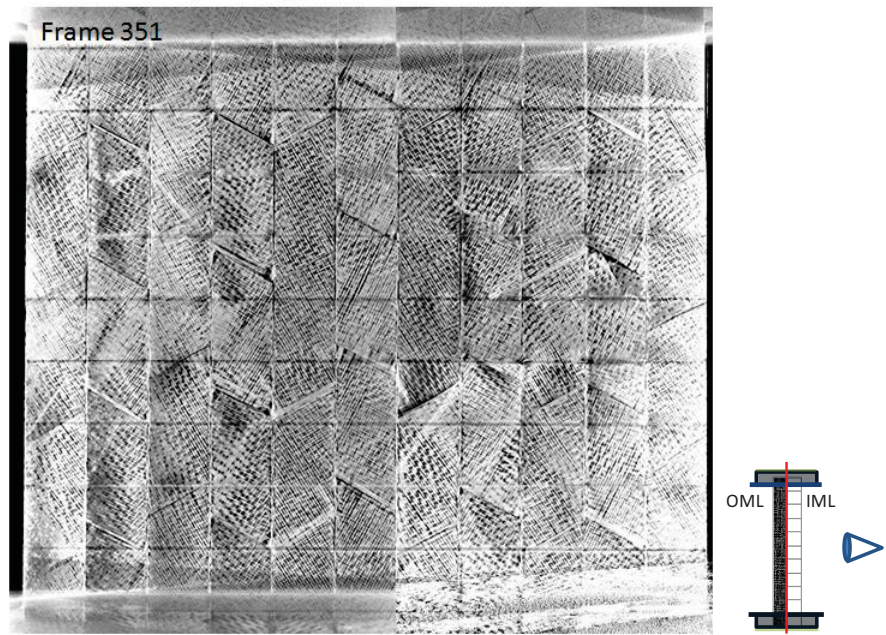
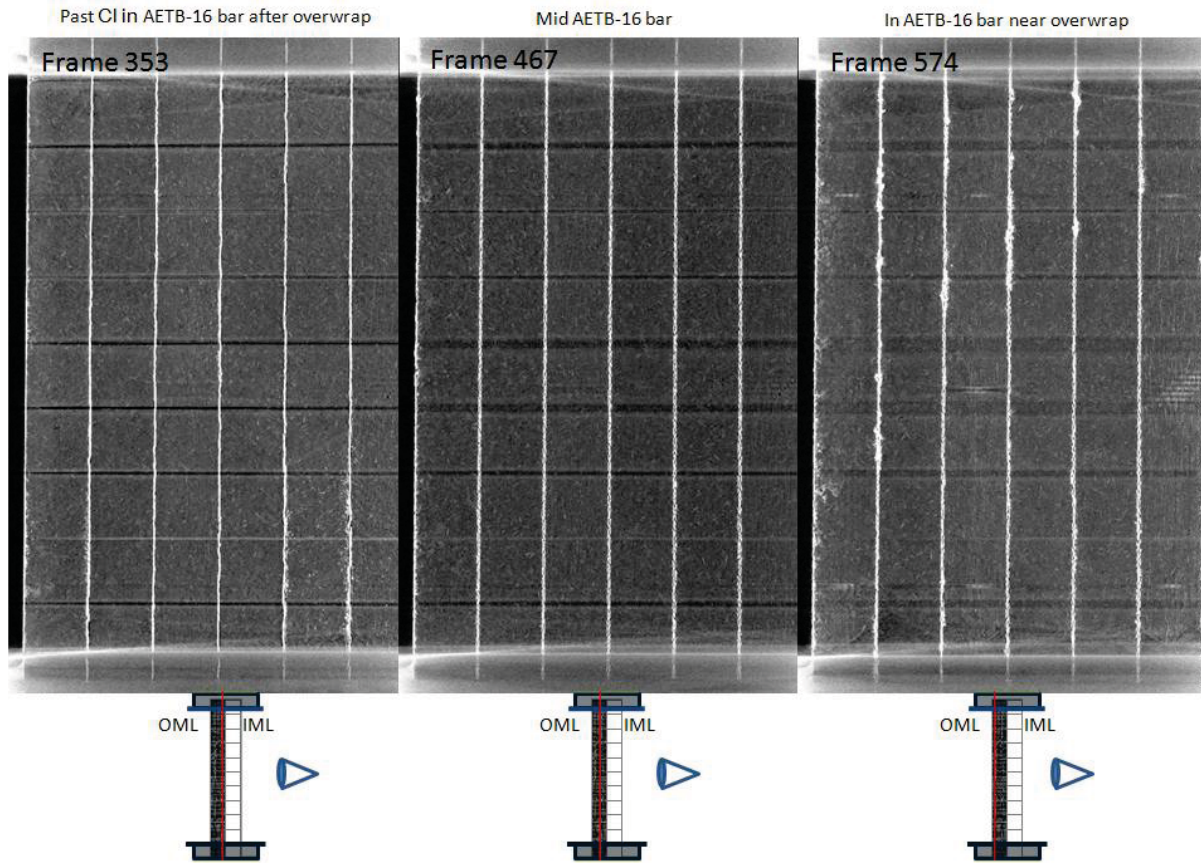


Figure B-3. Through Panel Thickness - CT Images of SITPS-0 (continued)

Partial View of Panel



Overwrap on longitudinal AETB-16 bars

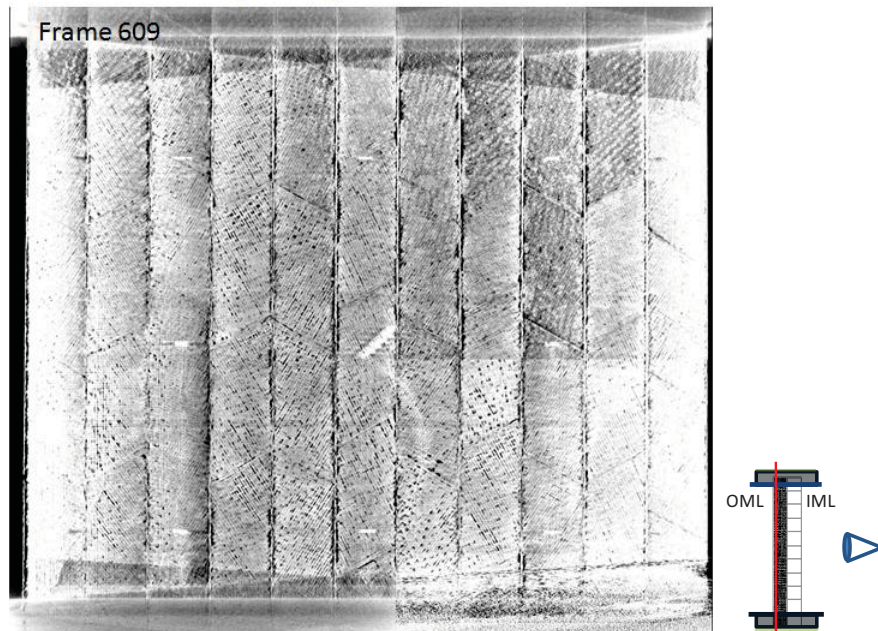


Figure B-3. Through Panel Thickness - CT Images of SITPS-0 (continued)

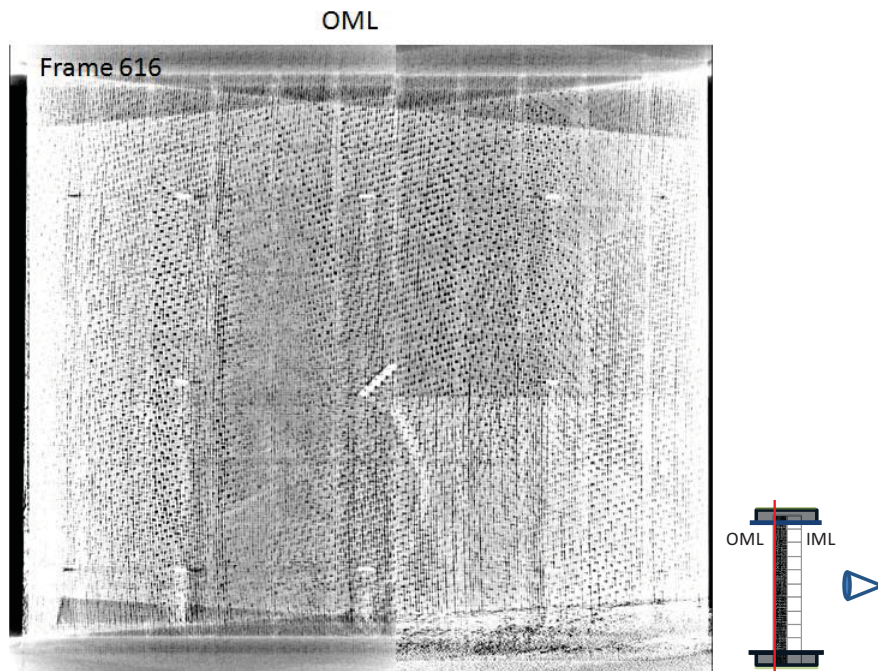
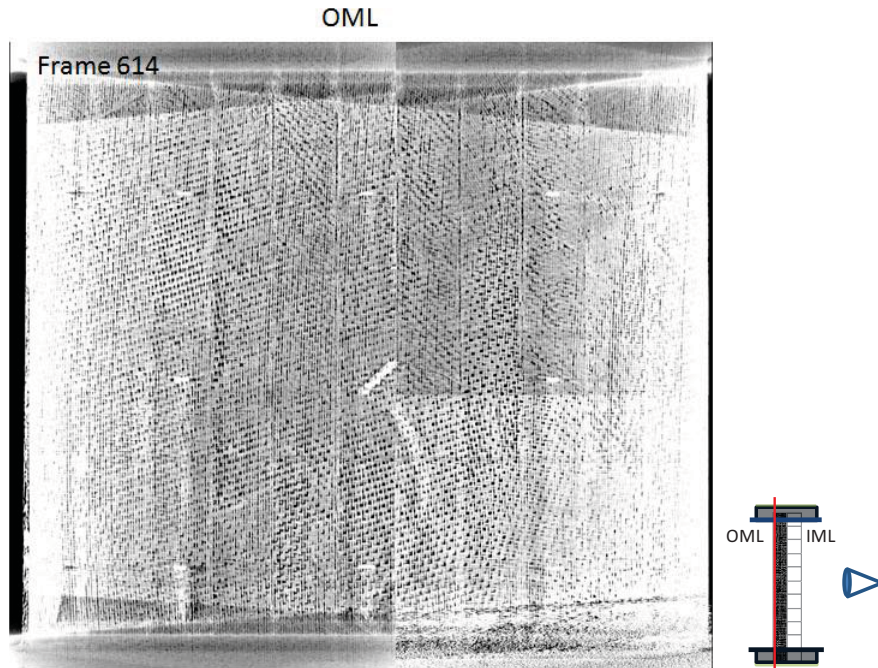


Figure B-3. Through Panel Thickness - CT Images of SITPS-0 (continued))

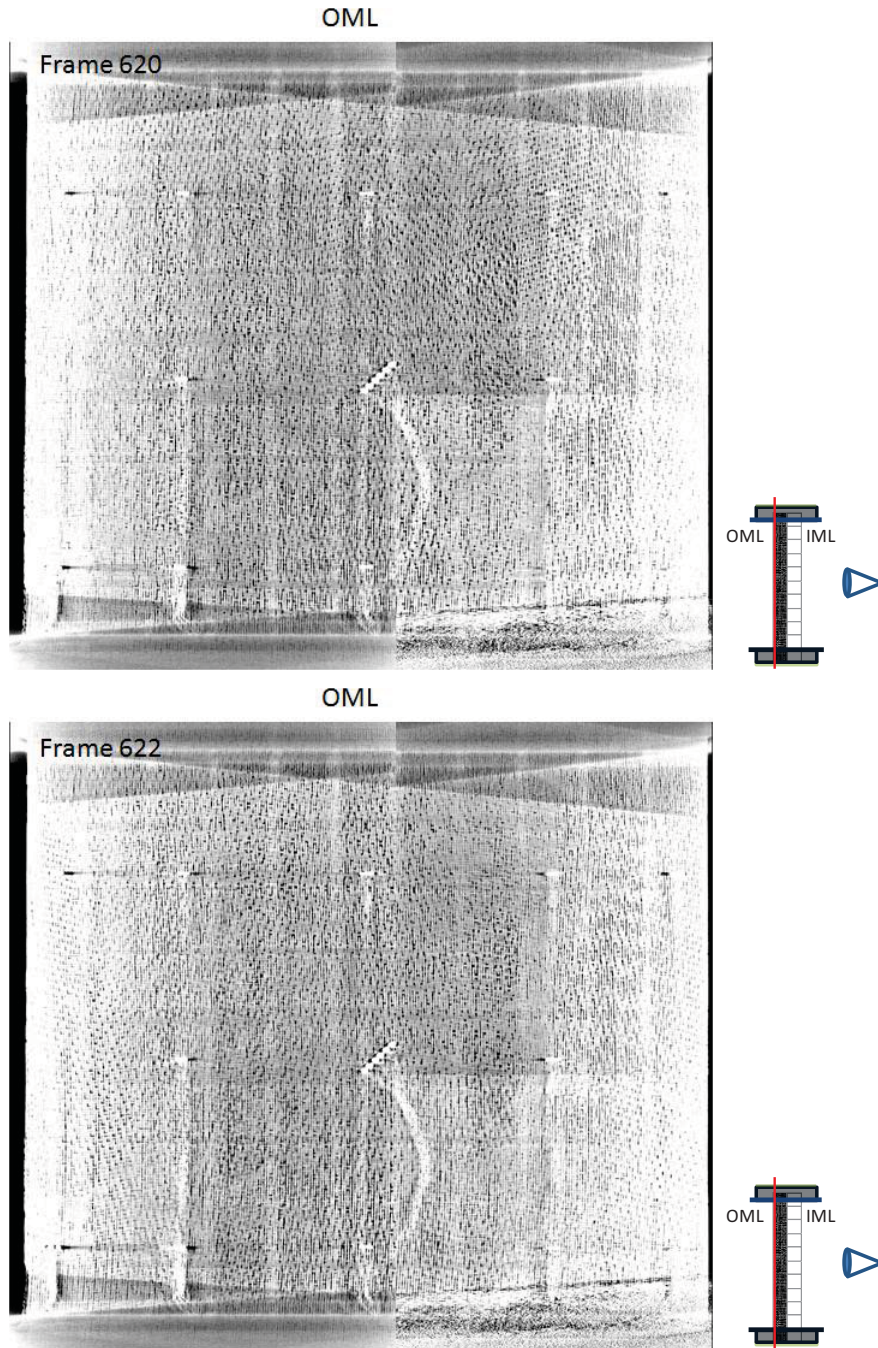


Figure B-3. Through Panel Thickness - CT Images of SITPS-0 (continued)

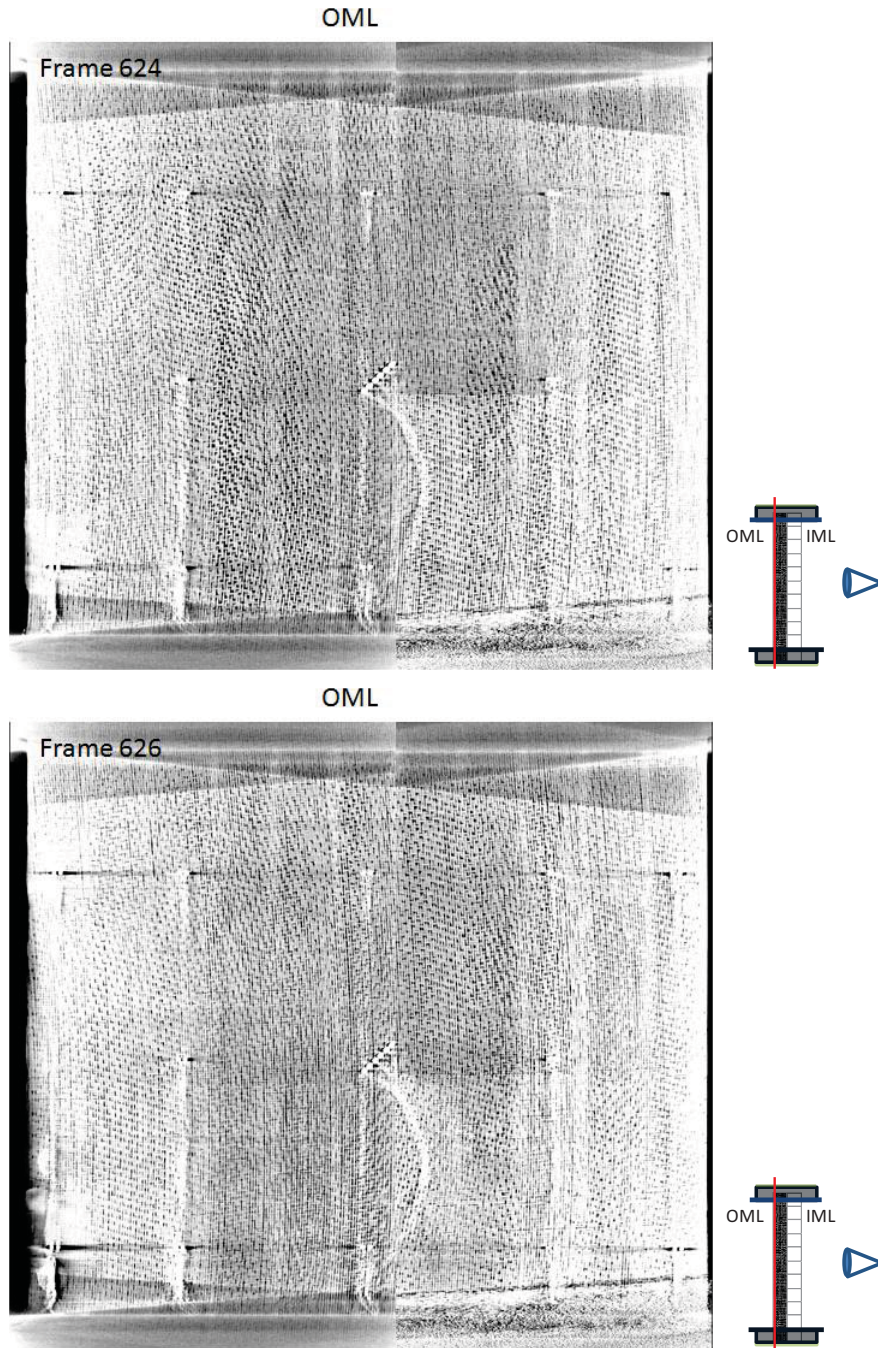
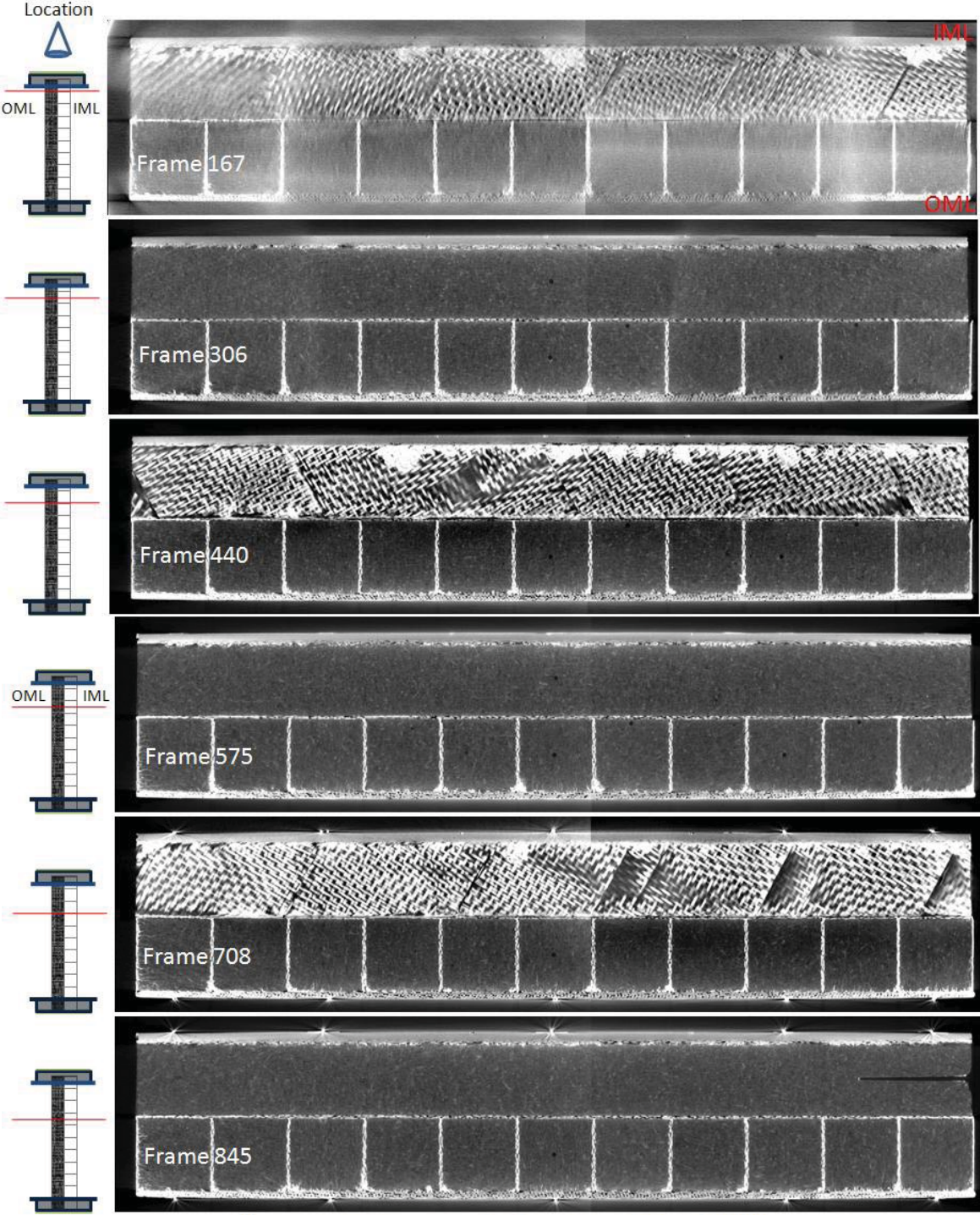


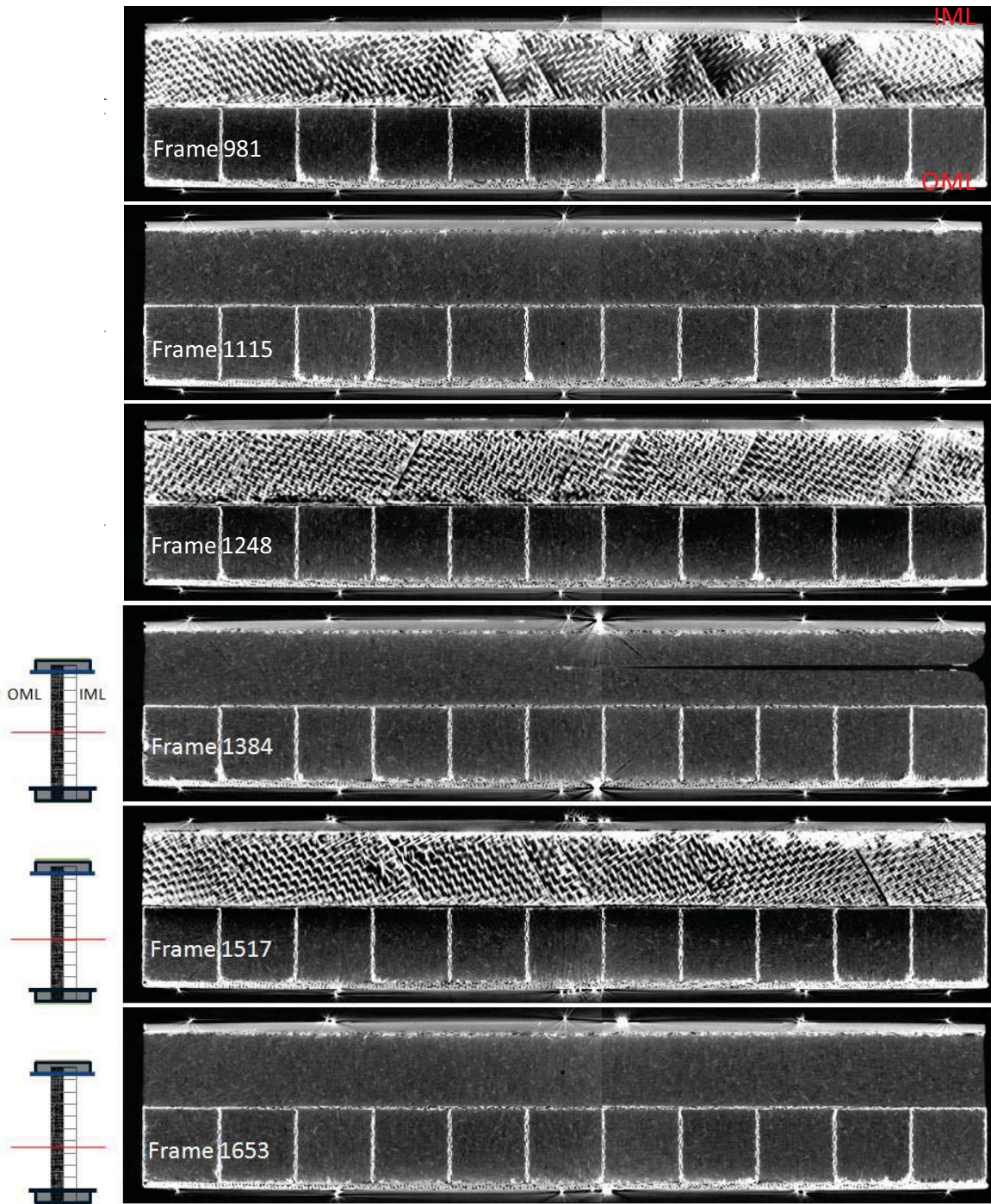
Figure B-3. Through Panel Thickness - CT Images of SITPS-0 (continued)

B.3 Through Panel Depth - CT Images of SITPS-0



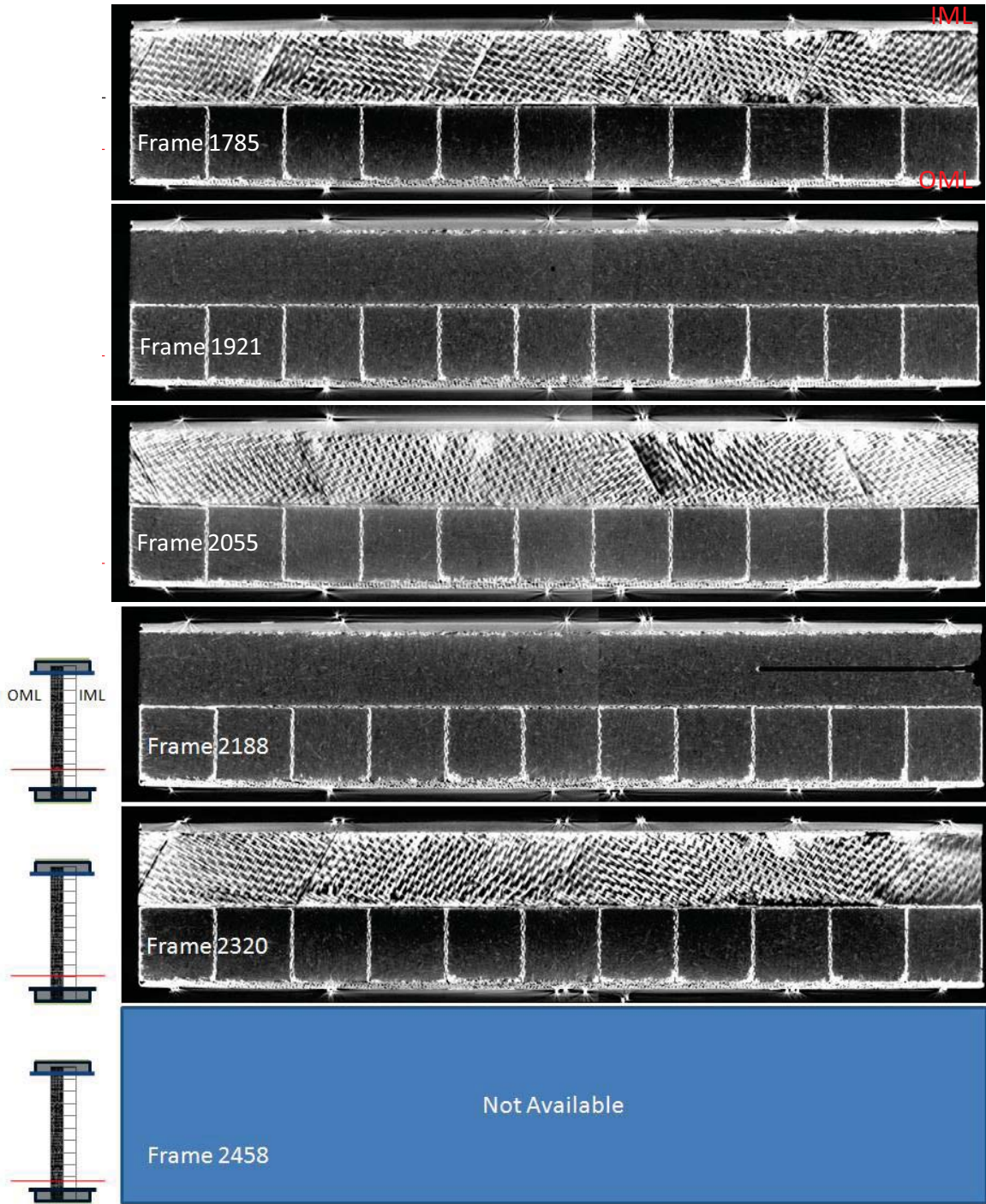
Note: Voids along intersection of overwrap and lower AETB bars
 Variation in porosity along OML (S200H)

Figure B-4. Through Panel Depth - CT Images of SITPS-0



Note: Voids along intersection of overwrap and lower AETB bars
 Variation in porosity along OML (S200H)

Figure B-4. Through Panel Depth - CT Images of SITPS-0 (continued)



Note: Voids along intersection of overwrap and lower AETB bars
 Variation in porosity along OML (S200H)

Figure B-4. Through Panel Depth - CT Images of SITPS-0 (continued)

The voids along the intersection of the overwrap and the lower AETB bars were seen both pre- and post- compression testing.

REPORT DOCUMENTATION PAGE

*Form Approved
OMB No. 0704-0188*

The public reporting burden for this collection of information is estimated to average 1 hour per response, including the time for reviewing instructions, searching existing data sources, gathering and maintaining the data needed, and completing and reviewing the collection of information. Send comments regarding this burden estimate or any other aspect of this collection of information, including suggestions for reducing this burden, to Department of Defense, Washington Headquarters Services, Directorate for Information Operations and Reports (0704-0188), 1215 Jefferson Davis Highway, Suite 1204, Arlington, VA 22202-4302. Respondents should be aware that notwithstanding any other provision of law, no person shall be subject to any penalty for failing to comply with a collection of information if it does not display a currently valid OMB control number.
PLEASE DO NOT RETURN YOUR FORM TO THE ABOVE ADDRESS.

1. REPORT DATE (DD-MM-YYYY) 01-07-2011		2. REPORT TYPE Contractor Report		3. DATES COVERED (From - To)	
4. TITLE AND SUBTITLE Edgewise Compression Testing of SITPS-0 (Structurally Integrated Thermal Protection System)				5a. CONTRACT NUMBER NNL09AM18T	
				5b. GRANT NUMBER	
				5c. PROGRAM ELEMENT NUMBER	
6. AUTHOR(S) Brewer, Amy R.				5d. PROJECT NUMBER	
				5e. TASK NUMBER	
				5f. WORK UNIT NUMBER 599489.02.07.07.02	
7. PERFORMING ORGANIZATION NAME(S) AND ADDRESS(ES) NASA Langley Research Center Hampton, VA 23681-2199				8. PERFORMING ORGANIZATION REPORT NUMBER	
9. SPONSORING/MONITORING AGENCY NAME(S) AND ADDRESS(ES) National Aeronautics and Space Administration Washington, DC 20546-0001				10. SPONSOR/MONITOR'S ACRONYM(S) NASA	
				11. SPONSOR/MONITOR'S REPORT NUMBER(S) NASA/CR-2011-217161	
12. DISTRIBUTION/AVAILABILITY STATEMENT Unclassified - Unlimited Subject Category 34 Availability: NASA CASI (443) 757-5802					
13. SUPPLEMENTARY NOTES Langley Technical Monitor: Kim S. Bey					
14. ABSTRACT The Structurally Integrated Thermal Protection System (SITPS) task was initiated by the NASA Hypersonics Project under the Fundamental Aeronautics Program to develop a structural load-carrying thermal protection system for use in aerospace applications. The initial NASA concept for SITPS consists of high-temperature composite facesheets (outer and inner mold lines) with a light-weight insulated structural core. An edgewise compression test was performed on the SITPS-0 test article at room temperature using conventional instrumentation and methods in order to obtain panel-level mechanical properties and behavior of the panel. Three compression loadings (10, 20 and 37 kips) were applied to the SITPS-0 panel. The panel behavior was monitored using standard techniques and non-destructive evaluation methods such as photogrammetry and acoustic emission. The elastic modulus of the SITPS-0 panel was determined to be 1.146x106 psi with a proportional limit at 1039 psi. Barrel-shaped bending of the panel and partial delamination of the IML occurred under the final loading.					
15. SUBJECT TERMS compression, mechanical testing, STIPS, structurally integrated thermal protection, TPS					
16. SECURITY CLASSIFICATION OF:			17. LIMITATION OF ABSTRACT	18. NUMBER OF PAGES	19a. NAME OF RESPONSIBLE PERSON
a. REPORT	b. ABSTRACT	c. THIS PAGE			STI Help Desk (email: help@sti.nasa.gov)
U	U	U	UU	51	19b. TELEPHONE NUMBER (Include area code) (443) 757-5802